

1 **Boosting with Omicron-matched or historical mRNA vaccines increases**  
2 **neutralizing antibody responses and protection against B.1.1.529 infection in**  
3 **mice**

4  
5  
6 Baoling Ying<sup>1\*</sup>, Suzanne M. Scheaffer<sup>1\*</sup>, Bradley Whitener<sup>1\*</sup>, Chieh-Yu Liang<sup>1,2</sup>, Oleksandr  
7 Dmytrenko<sup>1</sup>, Samantha Mackin<sup>1,2</sup>, Kai Wu<sup>3</sup>, Diana Lee<sup>3</sup>, Laura E. Avena<sup>3</sup>, Zhenlu Chong<sup>1</sup>,  
8 James Brett Case<sup>1</sup>, LingZhi Ma<sup>3</sup>, Thu Kim<sup>3</sup>, Caralyn Sein<sup>3</sup>, Angela Woods<sup>3</sup>, Daniela Montes  
9 Berrueta<sup>3</sup>, Andrea Carfi<sup>3</sup>, Sayda M. Elbashir<sup>3</sup>, Darin K. Edwards<sup>3</sup>, Larissa B. Thackray<sup>1¶</sup>, and  
10 Michael S. Diamond<sup>1,2,4,5,6 ¶‡</sup>

11  
12  
13 <sup>1</sup>Department of Medicine, Washington University School of Medicine, St. Louis, MO 63110, USA

14 <sup>2</sup>Department of Pathology & Immunology, Washington University School of Medicine, St. Louis, MO, USA

15 <sup>3</sup>Moderna, Inc., Cambridge MA, USA

16 <sup>4</sup>Department of Molecular Microbiology, Washington University School of Medicine, St. Louis, MO, USA

17 <sup>5</sup>The Andrew M. and Jane M. Bursky Center for Human Immunology and Immunotherapy Programs,  
18 Washington University School of Medicine. St. Louis, MO, USA

19 <sup>6</sup>Center for Vaccines and Immunity to Microbial Pathogens, Washington University School of Medicine,  
20 Saint Louis, MO, USA

21  
22 \*Equal contributors

23 ¶ Corresponding authors: Larissa B. Thackray, Ph.D. ([lthackray@wustl.edu](mailto:lthackray@wustl.edu)) and Michael S.  
24 Diamond, M.D., Ph.D. ([diamond@wusm.wustl.edu](mailto:diamond@wusm.wustl.edu))

25 Lead Contact: Michael S. Diamond, M.D., Ph.D.

26 **ABSTRACT**

27           The B.1.1.529 Omicron variant jeopardizes vaccines designed with early pandemic spike  
28 antigens. Here, we evaluated in mice the protective activity of the Moderna mRNA-1273 vaccine  
29 against B.1.1.529 before or after boosting with preclinical mRNA-1273 or mRNA-1273.529, an  
30 Omicron-matched vaccine. Whereas two doses of mRNA-1273 vaccine induced high levels of  
31 serum neutralizing antibodies against historical WA1/2020 strains, levels were lower against  
32 B.1.1.529 and associated with infection and inflammation in the lung. A primary vaccination  
33 series with mRNA-1273.529 potently neutralized B.1.1.529 but showed limited inhibition of  
34 historical or other SARS-CoV-2 variants. However, boosting with mRNA-1273 or mRNA-  
35 1273.529 vaccines increased serum neutralizing titers and protection against B.1.1.529  
36 infection. Nonetheless, the levels of inhibitory antibodies were higher, and viral burden and  
37 cytokines in the lung were slightly lower in mice given the Omicron-matched mRNA booster.  
38 Thus, in mice, boosting with mRNA-1273 or mRNA-1273.529 enhances protection against  
39 B.1.1.529 infection with limited differences in efficacy measured.

## 40 INTRODUCTION

41 Since the inception of the SARS-CoV-2 pandemic in late 2019, almost 400 million  
42 infections and 5.8 million deaths have been recorded (<https://covid19.who.int>). Several highly  
43 effective vaccines targeting the SARS-CoV-2 spike protein encompassing multiple platforms  
44 ((lipid nanoparticle encapsulated mRNA, inactivated virion, or viral-vectored vaccine platforms  
45 (Graham, 2020)) were developed and deployed rapidly with billions of doses administered  
46 (<https://covid19.who.int>). These vaccines use the SARS-CoV-2 spike protein from historical  
47 strains that circulated during the early phases of the pandemic in 2020 and have reduced the  
48 numbers of infections, hospitalizations, and COVID-19-related deaths. Despite the success of  
49 COVID-19 vaccines, the continued evolution of more transmissible SARS-CoV-2 variants with  
50 amino acid substitutions, deletions, and insertions in the spike protein jeopardizes the efficacy of  
51 global vaccination campaigns (Krause et al., 2021).

52 The SARS-CoV-2 spike protein engages angiotensin-converting enzyme 2 (ACE2) on the  
53 surface of human cells to facilitate entry and infection (Letko et al., 2020). The S1 fragment of  
54 the spike protein contains the N-terminal (NTD) and receptor binding (RBD) domains, which are  
55 targets of neutralizing monoclonal (Barnes et al., 2020; Cao et al., 2020; Pinto et al., 2020;  
56 Tortorici et al., 2020; Zost et al., 2020) and polyclonal antibodies (Rathe et al., 2020). In late  
57 November of 2021, the Omicron (B.1.1.529) variant emerged, which has the largest number  
58 (>30) of amino acid substitutions, deletions, or insertions in the spike protein described to date.  
59 These changes in the spike raise concerns for escape from protection by existing vaccines that  
60 target early pandemic spike proteins. Indeed, reduced serum neutralization of B.1.1.529 virus  
61 (Edara et al., 2021; Pajon et al., 2022) and large numbers of symptomatic breakthrough  
62 infections with B.1.1.529 have been reported in vaccinated individuals (Buchan et al., 2022;  
63 Christensen et al., 2022; Elliott et al., 2021).

64 Here, we evaluated the antibody responses and protective activity against B.1.1.529  
65 Omicron virus of a preclinical version of the current Moderna vaccine, mRNA-1273, or an

66 Omicron-targeted vaccine, mRNA-1273.529, designed with sequences from the historical  
67 Wuhan-1 or B.1.1.529 spike genes, respectively, in the context of a primary (two-dose)  
68 immunization series or third-dose boosters. We hoped to define serum antibody correlates of  
69 protection against B.1.1.529, determine the likelihood and significance of breakthrough  
70 infections, define the differences in immunogenicity and protection of homologous and  
71 heterologous mRNA vaccine boosters, and evaluate the activity of mRNA-1273.529 in the  
72 context of a primary immunization series against historical and variants of concern strains that  
73 emerged prior to Omicron.

74         After a primary immunization series, mRNA-1273.529 induced antibody responses that  
75 efficiently neutralized viruses displaying B.1.1.529 spike proteins but poorly inhibited infection of  
76 viruses expressing spike proteins of a historical strain or key variants (e.g., Beta (B.1.351) and  
77 Delta (B.1.617.2)). Whereas a primary immunization series with a high-dose mRNA-1273  
78 formulation conferred protection against both historical and B.1.1.529 viruses, a low-dose  
79 series, which induced levels of neutralizing antibodies against WA1/2020 strains that  
80 correspond to those measured in human serum (Wu et al., 2021), protected against WA1/2020  
81 but did not control viral infection or inflammation in the lungs of B.1.1.529-challenged mice.  
82 Boosting with either mRNA-1273 or Omicron-matched mRNA-1273.529 vaccine increased  
83 levels of neutralizing antibodies and protection against B.1.1.529, although higher levels of  
84 neutralizing antibodies and lower levels of lung infection and inflammation were observed in  
85 mice boosted with mRNA-1273.529. Thus, the levels of vaccine-induced immunity that protect  
86 against historical or other variant SARS-CoV-2 strains (Ying et al., 2021) fail to prevent  
87 breakthrough infection by B.1.1.529 virus, necessitating boosting with either matched or  
88 unmatched vaccines.

89

## 90 RESULTS

91           **Antibody responses against B.1.1.529 in K18-hACE2 mice.** We evaluated the  
92 antibody response against B.1.1.529 after immunization with a preclinical version of mRNA-  
93 1273 that encodes for the prefusion-stabilized spike protein of SARS-CoV-2 Wuhan-1 strain  
94 (Corbett et al., 2020). We used K18-hACE2 transgenic mice, which are susceptible to severe  
95 infection after intranasal inoculation by many SARS-CoV-2 strains (Chen et al., 2021b; Winkler  
96 et al., 2020). Groups of 7-week-old female K18-hACE2 mice were immunized twice over three  
97 weeks by intramuscular route with 5 or 0.1  $\mu$ g doses of mRNA-1273 or a control mRNA vaccine  
98 (**Fig 1A**). A lower vaccine dose arm was included for evaluating correlates of protection, as we  
99 expected breakthrough infections in this group. Serum samples were collected three weeks  
100 after the second dose, and IgG responses against spike proteins (Wuhan-1 and B.1.1.529) were  
101 evaluated by ELISA. We confirmed that equivalent amounts of antigenically intact Wuhan-1 and  
102 B.1.1.529 spike (proline-stabilized, S2P) and RBD proteins were adsorbed based on detection  
103 with sarbecovirus cross-reactive monoclonal antibodies (VanBlargan et al., 2021) (**Fig 1B**).  
104 Antibody responses against both the Wuhan-1 and B.1.1.529 spike proteins were robust after  
105 two immunizations with mRNA-1273. For the 5  $\mu$ g dose, mean serum endpoint titers ranged  
106 from ~4,000,000 to 800,000 against the Wuhan-1 and B.1.1.529 spike proteins and 1,000,000  
107 and 40,000 for the Wuhan-1 and B.1.1.529 RBD, respectively (**Fig 1C-D**). For the 0.1  $\mu$ g dose,  
108 approximately 10-fold lower serum IgG responses against the spike and RBD proteins were  
109 measured (**Fig 1E-F**). The most noticeable difference in IgG responses after mRNA-1273  
110 vaccination was the reduced titer against the B.1.1.529 RBD compared to Wuhan-1 RBD  
111 protein (**Fig 1D and F**).

112           We characterized functional antibody responses by measuring the inhibitory effects of  
113 serum on SARS-CoV-2 infectivity using a focus-reduction neutralization test (FRNT) (Case et  
114 al., 2020b) and fully-infectious SARS-CoV-2 WA1/2020 D614G and B.1.1.529 strains (**Fig 1G-H**

115 **and S1**). Due to the limited amount of sera recovered from live animals, we started dilutions at  
116 1/60, which is just above the estimated level of neutralizing antibodies associated with  
117 protection in humans (Khoury et al., 2021). For the 5 µg dose, the mRNA-1273 vaccine induced  
118 robust serum neutralizing antibody responses against both WA1/2020 D614G and B.1.1.529  
119 (**Fig 1G-H and S1**). However, the geometric mean titers (GMTs) of neutralization were ~8-fold  
120 lower ( $P < 0.001$ ) against B.1.1.529, which agrees with data from human antibodies (Cameroni  
121 et al., 2021; Cao et al., 2021; Cele et al., 2021; Dejnirattisai et al., 2022; VanBlargan et al.,  
122 2022; Wilhelm et al., 2021). For the 0.1 µg mRNA-1273 vaccine dose, we observed ~8-fold less  
123 ( $P < 0.01$ ) serum neutralizing activity against WA1/2020 D614G compared to the higher vaccine  
124 dose. Serum from mRNA-1273-vaccinated mice with the 0.1 µg dose also showed large (>20-  
125 fold,  $P < 0.001$ ) reductions in neutralization of B.1.1.529, with all values assigned to the 1/60  
126 limit of detection (**Fig 1H**).

127 **Protection against B.1.1.529 by mRNA-1273 in K18-hACE2 mice.** We evaluated the  
128 protective activity of the mRNA-1273 vaccine against B.1.1.529 challenge. Although B.1.1.529  
129 is less pathogenic in mice and hamsters (Bentley et al., 2021; Halfmann et al., 2022; Shuai et  
130 al., 2022), the virus still replicates to reasonably high levels (approximately 10-100 million  
131 copies of *N* gene/mg at 6 days post-infection (dpi)) in the lungs of K18-hACE2 mice (Halfmann  
132 et al., 2022). Five weeks after the second vaccine dose, mice were challenged via intranasal  
133 route with  $10^4$  focus-forming units (FFU) of WA1/2020 D614G or B.1.1.529. Compared to the  
134 control mRNA vaccine, the 5 and 0.1 µg doses of mRNA-1273 vaccines prevented weight loss  
135 at 6 dpi after WA1/2020 D614G infection (**Fig 2A-B**). However, as B.1.1.529-challenged mice  
136 failed to lose weight, we could not use this metric to evaluate the protective activity of the  
137 mRNA-1273 vaccine.

138 We next compared the levels of WA1/2020 D614G and B.1.1.529 infection in control  
139 mRNA-vaccinated K18-hACE2 mice at 6 dpi (**Fig 2C-H**). In the nasal washes of control mRNA-

140 vaccinated K18-hACE2 mice, although some variability was observed, moderate amounts ( $10^5$   
141 to  $10^6$  copies of *N* per mL) of WA1/2020 D614G RNA were measured; approximately 10-fold  
142 lower levels ( $10^4$  to  $10^5$  copies of *N* per mL) were measured after challenge with B.1.1.529 (**Fig**  
143 **2C and F**). In the nasal turbinates, a similar pattern was seen with approximately 100-fold lower  
144 levels of B.1.1.529 RNA ( $\sim 10^3$  versus  $10^5$  copies of *N* per mg) (**Fig 2D and G**). In the lungs of  
145 control mRNA-vaccinated K18-hACE2 mice, approximately 10-fold less B.1.1.529 RNA was  
146 measured compared to WA1/2020 D614G RNA (**Fig 2E and H**).

147 We assessed the effects of mRNA-1273 vaccination on WA1/2020 D614G and  
148 B.1.1.529 infection in respiratory tract samples. The 5  $\mu\text{g}$  dose of mRNA-1273 vaccine protected  
149 against WA1/2020 D614G infection with little viral RNA detected at 6 dpi (**Fig 2C-E**). In  
150 comparison, while B.1.1.529 viral RNA was not detected in the nasal washes or nasal turbinates  
151 of animals immunized with 5  $\mu\text{g}$  of mRNA-1273, we observed breakthrough infection, albeit at  
152 low levels, in the lungs of most (5 of 8) animals (**Fig 2C-E**). Although the 0.1  $\mu\text{g}$  dose of mRNA-  
153 1273 vaccine conferred protection against WA1/2020 D614G, several animals had viral RNA in  
154 nasal washes (4 of 7 mice), nasal turbinates (7 of 7), and lungs (5 of 7 mice). However, these  
155 breakthrough infections generally had reduced (100-100,000-fold) levels compared to the  
156 control mRNA vaccine (**Fig 2F-H**). After immunization with 0.1  $\mu\text{g}$  of mRNA-1273, B.1.1.529  
157 infection levels were lower in the nasal washes but not in the nasal turbinates (**Fig 2F-G**), in part  
158 due to the lower levels of viral RNA in the control mRNA-vaccinated samples. However, in the  
159 lungs, 7 of 7 mice vaccinated with the 0.1  $\mu\text{g}$  dose sustained high levels of B.1.1.529  
160 breakthrough infection with  $\sim 10^6$  copies of *N* per mg, although some protection still was  
161 observed (**Fig 2H**).

162 Serum neutralizing antibody titers showed an inverse correlation with amounts of viral  
163 RNA in the lung (**Fig 2I**) for both viruses, with more infection occurring in B.1.1.529-infected  
164 animals with lower neutralization titers. The correlation was most linear for B.1.1.529-challenged

165 animals ( $R^2 = 0.8155$ ,  $P < 0.0001$ ), with a minimum neutralizing titer of approximately 2,000  
166 required to completely prevent infection at 6 dpi. Most of the breakthrough infections occurred  
167 with the lower 0.1  $\mu\text{g}$  dose of mRNA vaccines, which models what might be occurring in  
168 immunocompromised or elderly individuals, or immunocompetent individuals at times remote  
169 from completion of their primary immunization series (Chen et al., 2021a; Choi et al., 2021;  
170 Evans et al., 2021).

171 We tested whether the mRNA-1273 vaccine could suppress cytokine and chemokine  
172 responses in the lung at 6 dpi of K18-hACE2 mice after challenge with WA1/2020 D614G or  
173 B.1.1.529 (**Fig 3A-B**). WA1/2020 D614G or B.1.1.529 infection of control mRNA vaccinated  
174 K18-hACE2 mice resulted in increased expression of several pro-inflammatory cytokines and  
175 chemokines including G-CSF, GM-CSF,  $\text{IFN}\gamma$ ,  $\text{IL-1}\beta$ , IL-6, CXCL1, CXCL5, CXCL9, CXCL10,  
176 CCL2, CCL4, and  $\text{TNF-}\alpha$  in lung homogenates (**Table S1 and S2**). Pro-inflammatory cytokine  
177 and chemokines in the lung at 6 dpi generally were lower in animals vaccinated with 5  $\mu\text{g}$  dose  
178 of mRNA-1273 after challenge with WA1/2020 D614G or B.1.1.529 (**Fig 3A**). Although K18-  
179 hACE2 mice immunized with the lower 0.1  $\mu\text{g}$  dose also showed diminished levels of cytokines  
180 and chemokines after WA1/2020 D614G infection, this protection was not observed after  
181 B.1.1.529 challenge; levels of pro-inflammatory cytokines in the lung were similar in mice  
182 immunized with the 0.1  $\mu\text{g}$  dose control and mRNA-1273 vaccines after challenge with  
183 B.1.1.529 (**Fig 3B**).

184 We performed histological analysis of lung tissues from immunized animals challenged  
185 with WA1/2020 D614G or B.1.1.529. Lung sections obtained at 6 dpi from mice immunized with  
186 either dose of control mRNA vaccine and challenged with WA1/2020 D614G showed severe  
187 pneumonia characterized by immune cell infiltration, alveolar space consolidation, vascular  
188 congestion, and interstitial edema (**Fig 3C-D**). In comparison, K18-hACE2 mice immunized with  
189 the control mRNA vaccines and challenged with B.1.1.529 showed less lung pathology, with



190 focal airspace consolidation and immune cell infiltration, results that are consistent with the  
191 lower pathogenicity of B.1.1.529 in rodents (Abdelnabi et al., 2021; Bentley et al., 2021;  
192 Halfmann et al., 2022; Shuai et al., 2022).

193 Mice immunized with the high or low dose of mRNA-1273 and challenged with  
194 WA1/2020 D614G did not develop lung pathology, with histological findings similar to uninfected  
195 mice (**Fig 3C-E**). Mice immunized with the high dose of mRNA-1273 vaccine were protected  
196 against the mild pathological changes associated with B.1.1.529 infection (**Fig 3C**). However,  
197 animals immunized with the lower dose of mRNA-1273 showed similar lung pathology after  
198 B.1.1.529 infection as control mRNA-vaccinated animals, with patchy immune cell infiltration,  
199 airway space thickening, and mild alveolar congestion (**Fig 3D**).

200 **Effects of an mRNA-1273 booster dose on antibody responses and protection in**  
201 **K18-hACE2 mice.** As booster doses are now used in humans to augment immunity and  
202 protection against variants, including B.1.1.529 (Atmar et al., 2022; Bar-On et al., 2021; Pajon et  
203 al., 2022), we evaluated their effects in K18-hACE2 mice. A cohort of 7-week-old female K18-  
204 hACE2 mice was immunized with a primary series over a 3-week interval with either a 5 or 0.25  
205  $\mu\text{g}$  dose of mRNA-1273 or a control vaccine (**Fig 4A**). The 0.25  $\mu\text{g}$  dose used was higher than  
206 the 0.1  $\mu\text{g}$  dose used above, in part due to the extended interval between the primary  
207 immunization series and boosting. After a 17 to 19-week rest period, blood was collected (pre-  
208 boost), animals were boosted with 1  $\mu\text{g}$  of mRNA-1273 or a control vaccine, a second bleed  
209 (post-boost) was performed one month later (**Fig 4A**), and sera were tested for neutralizing  
210 activity. As expected, 5- to 10-fold lower pre-boost neutralizing titers were observed from  
211 animals immunized with the 0.25  $\mu\text{g}$  than the 5  $\mu\text{g}$  dose of mRNA-1273 (**Fig 4B-E and Fig S2**).  
212 While the titers against WA1/2020 D614G were high (GMT: 9,579, 5  $\mu\text{g}$ ; 3,096, 0.25  $\mu\text{g}$ ), we  
213 observed 10- to 20-fold lower levels ( $P < 0.01$ , 5  $\mu\text{g}$ ) of neutralizing antibodies against  
214 B.1.1.529, with half of the sera from mice vaccinated with the 0.25  $\mu\text{g}$  formulation showing no

215 inhibitory activity at the 1/60 limit of detection of the assay (**Fig 4B, D and Fig S2**). One month  
216 after boosting with mRNA-1273, serum neutralizing titers rose against both viruses (**Fig 4C, E**  
217 **and Fig S2**). All mice boosted with mRNA-1273 had neutralizing titers against B.1.1.529 above  
218 the estimated threshold (titer of 50) for protection (GMT: 6,124, 5 µg; 1,161, 0.25 µg).

219 We evaluated the protective effects of mRNA-1273 boosting on B.1.1.529 infection by  
220 measuring viral RNA levels in nasal wash, nasal turbinates, and lungs at 6 dpi (**Fig 4F-G**).  
221 Compared to animals immunized and boosted with the control mRNA vaccine, K18-hACE2 mice  
222 vaccinated with the 5 or 0.25 µg primary series and boosted with mRNA-1273 showed reduced  
223 levels ( $P < 0.001$ ) of B.1.1.529 viral RNA in the respiratory tract, with little to no detectable *N*  
224 gene copies in the nasal wash or turbinates. However, breakthrough infection, albeit at 2,500 to  
225 6,000-fold lower levels ( $P < 0.001$ ) than the control vaccine, was detected in the lungs of the  
226 majority (8 of 12) of mRNA-1273 boosted K18-hACE2 mice (**Fig 4F-G**). Thus, boosting of mice  
227 with mRNA-1273 vaccine, despite not being matched to the challenge virus, improves  
228 neutralizing antibody responses and reduces infection by B.1.1.529 in the upper and lower  
229 respiratory tracts.

230 **Immunogenicity of an Omicron-matched mRNA vaccine.** As an alternative to a third  
231 dose of mRNA-1273, boosting with vaccines targeting the B.1.1.529 spike might provide  
232 enhanced immunity and protection. To begin to address this question, we generated a lipid-  
233 encapsulated mRNA vaccine (mRNA-1273.529) encoding a proline-stabilized SARS-CoV-2  
234 spike from the B.1.1.529 virus. As a first test of its activity, we immunized BALB/c mice twice at  
235 3-week intervals with 1 or 0.1 µg of mRNA 1273 or mRNA 1273.529 vaccines (**Fig 5A**). Three  
236 weeks after the first dose (Day 21) and two weeks after the second dose (Day 36), serum was  
237 collected (**Fig 5A**) and analyzed for binding to Wuhan-1 and B.1.1.529 spike proteins by ELISA  
238 (**Fig 5B**). At day 21 after the first dose, animals receiving 1 µg of mRNA-1273 showed  
239 approximately 11-fold higher levels of binding to homologous Wuhan-1 than heterologous

240 B.1.1.529 spike, whereas equivalent responses to Wuhan-1 and B.1.1.529 spike proteins were  
241 detected after vaccination with 1  $\mu$ g of mRNA-1273.529. In comparison, mice receiving the  
242 lower 0.1  $\mu$ g dose of either mRNA-1273 or mRNA-1273.529 had low levels (near the limit of  
243 detection) of anti-spike antibody at day 21. Serum collected two weeks after the second dose of  
244 mRNA-1273 or mRNA-1273.529 also was tested for binding to Wuhan-1 and B.1.1.529 spike  
245 proteins. Immunization with either dose of mRNA-1273 resulted in higher (8 to 20-fold) serum  
246 IgG binding titers to Wuhan-1 than B.1.1.529 spike (**Fig 5B**). Reciprocally higher levels (3-fold)  
247 of serum IgG binding to B.1.1.529 than Wuhan-1 spike were seen after two 0.1  $\mu$ g doses of  
248 mRNA-1273.529; however, immunization with two 1  $\mu$ g doses of mRNA-1273.529 resulted in  
249 equivalent serum antibody binding to Wuhan-1 and B.1.1.529 spike proteins.

250 We next tested the inhibitory activity of serum antibodies of BALB/c mice that received  
251 two 1  $\mu$ g doses of mRNA-1273 or mRNA-1273.529 using a vesicular stomatitis virus (VSV)-  
252 based pseudovirus neutralization assay and spike proteins of Wuhan-1 D614G, B.1.351,  
253 B.1.617.2, or B.1.1.529 (**Fig 5C**). Two weeks after the second vaccine dose, animals immunized  
254 with mRNA-1273 had high serum neutralizing titers against Wuhan-1 D614G (GMT: 4,967) with  
255 approximately four-fold reductions ( $P < 0.01$ ) against viruses displaying B.1.351 (GMT: 1,310)  
256 or B.1.617.2 (GMT: 1,549). However, and consistent with data in K18-hACE2 mice (**Fig 4D**) and  
257 humans (Dejnirattisai et al., 2022; Liu et al., 2021a), BALB/c mice vaccinated with mRNA-1273  
258 had substantially lower (74-fold reduced, GMT:67,  $P < 0.01$ ) neutralizing titers against B.1.1.529  
259 with several samples falling near the presumed 1/50 threshold of protection. In comparison,  
260 animals immunized with two 1  $\mu$ g doses of the Omicron variant-targeted mRNA-1273.529  
261 vaccine showed a distinct pattern. Although high neutralization titers were observed against  
262 B.1.529 (GMT: 3,314), lower levels of neutralization (85 to 100-fold less,  $P < 0.01$ ) were  
263 detected against Wuhan-1 D614G (GMT: 33), B.1.351 (GMT: 39), and B.1.617.2 (GMT: 35),  
264 with most of the samples at the limit of detection of the neutralizing assay. Thus, and as

265 suggested recently in another preliminary study (Lee et al., 2022), a primary vaccination series  
266 with an Omicron-specific mRNA vaccine induces potently neutralizing antibodies against  
267 Omicron but not against historical viruses or other SARS-CoV-2 variants.

268 **Protective effects of an Omicron-targeted mRNA vaccine.** As BALB/c and K18-  
269 hACE2 mice immunized with a primary series were unavailable, we took advantage of an  
270 existing cohort of female 129S2 mice that had been immunized with a primary series over a 3-  
271 week interval with either a 5 or 0.25  $\mu$ g dose of mRNA-1273 or a control mRNA vaccine and  
272 then rested for 10 to 11 weeks (**Fig 6A**). Blood was collected (pre-boost sample), and groups of  
273 animals were boosted homologously or heterologously with 1  $\mu$ g of control mRNA, mRNA-1273,  
274 or mRNA-1273.529 vaccine, the same dose used in our BALB/c mouse studies above. Three to  
275 four weeks later, a second post-boost blood sample was collected (**Fig 6A**), and the neutralizing  
276 activity of pre- and post-boost serum antibodies were measured and compared. Mice that  
277 received 5 or 0.25  $\mu$ g doses of mRNA-1273 had high-levels (GMT: 29,161, 5  $\mu$ g; 5,749, 0.25  $\mu$ g)  
278 of pre-boost neutralizing antibodies against WA1/2020 N501Y/D614G (**Fig 6B and S3**). We  
279 used the WA1/2020 N501Y/D614G strain because the N501Y substitution enables engagement  
280 of murine ACE2 and productive infection of conventional strains of laboratory mice (Gu et al.,  
281 2020; Liu et al., 2021b; Rathnasinghe et al., 2021; Ying et al., 2021). However, mice that  
282 received 5 or 0.25  $\mu$ g doses of mRNA-1273 had 15- to 18-fold lower serum pre-boost  
283 neutralizing titers against B.1.1.529 (GMT: 1891, 5  $\mu$ g; 317, 0.25  $\mu$ g;  $P < 0.0001$ ) (**Fig 6B and**  
284 **S3**). One month after boosting with mRNA-1273 or mRNA-1273.529, neutralizing titers against  
285 WA1/2020 N501Y/D614G were approximately 2 to 6-fold-higher than before boosting (**Fig 6C-D**  
286 **and S3**). In comparison, boosting with mRNA-1273.529 resulted in 22 to 42-fold ( $P < 0.01$ )  
287 higher neutralizing titers against B.1.1.529, whereas the mRNA-1273 booster increased titers  
288 against B.1.1.529 by 2 to 5-fold ( $P < 0.05$ ) (**Fig 6C, E and Fig S3**). Thus, while both mRNA-

289 1273 and mRNA-1273.529 boosters augmented serum neutralizing activity of B.1.1.529, an  
290 Omicron-matched vaccine produced higher titers of neutralizing antibodies.

291 Three or four days after the post-boost bleed, 129S2 mice were challenged by the  
292 intranasal route with  $10^5$  FFU of WA1/2020 N501Y/D614G or B.1.1.529, and viral RNA levels at  
293 3 dpi were measured in the nasal washes, nasal turbinates, and lungs. B.1.1.529 is less  
294 pathogenic in 129S2 mice (Halfmann et al., 2022) with ~100-fold lower levels of viral RNA in the  
295 upper and lower respiratory tract than after WA1/2020 N501YD614G infection (**Fig 7A-B**).  
296 Nonetheless, substantial viral replication occurred allowing for evaluation of vaccine protection.  
297 Mice vaccinated with either 5 or 0.25  $\mu$ g doses of mRNA-1273 and boosted with either mRNA-  
298 1273 or mRNA-1273.529 showed almost complete protection against WA1/2020 N501Y/D614G  
299 infection in the nasal washes, nasal turbinates and lungs, with approximately 100,000- to  
300 1,000,000-fold reductions in viral RNA levels compared to mice immunized with control mRNA  
301 vaccine. Mice primed with the 5  $\mu$ g doses of mRNA-1273 and boosted with either mRNA-1273  
302 or mRNA-1273.529 analogously showed robust and equivalent protection against B.1.1.529  
303 infection (**Fig 7A**). In comparison, animals primed with the lower 0.25  $\mu$ g dose of mRNA-1273  
304 showed some differences after boosting and B.1.1.529 challenge (**Fig 7B**). Although B.1.1.529  
305 viral RNA levels were reduced in upper respiratory tract tissues after boosting with either  
306 mRNA-1273 or mRNA-1273.529, there was a trend ( $P = 0.07$ ) toward lower levels in the nasal  
307 turbinates in animals boosted with mRNA-1273.529. Moreover, a 27-fold reduction ( $P < 0.01$ ) in  
308 B.1.1.529 infection in the lungs was observed in mice boosted with the Omicron-matched  
309 mRNA-1273.529 compared to the mRNA-1273 vaccine.

310 As an independent metric of protection, we measured cytokine and chemokine levels in  
311 lung homogenates of the vaccinated and challenged 129S2 mice at 3 dpi (**Fig 7C-D and Table**  
312 **S3 and S4**). Mice immunized with 5 or 0.25  $\mu$ g doses of mRNA-1273 and then given a booster  
313 dose of either control, mRNA-1273, or mRNA-1273.529 vaccines generally showed lower levels

314 of pro-inflammatory cytokines and chemokines after WA1/2020 N501Y/D614G infection than  
315 animals that received three doses of control mRNA vaccine. In comparison, after B.1.1.529  
316 challenge several differences were noted: (a) the inflammatory response after B.1.1.529  
317 infection was lower in magnitude in control mRNA-vaccinated mice than after WA1/2020  
318 N501Y/D614G infection, consistent with its less pathogenic nature in 129 mice (Halfmann et al.,  
319 2022); (b) animals immunized with 5 µg doses of mRNA-1273 and then boosted with control,  
320 mRNA-1273, or mRNA-1273.529 vaccines showed reduced levels of cytokines and chemokines  
321 compared to those receiving three doses of control mRNA, indicating protection against  
322 inflammation by homologous or heterologous boosting (**Fig 7C**); and (c) mice immunized with  
323 two 0.25 µg doses of mRNA-1273 and boosted with control vaccine showed little reduction in  
324 cytokine and chemokine levels compared to mice receiving three doses of control mRNA  
325 vaccine following B.1.1.529 challenge (**Fig 7D**). While boosting with mRNA-1273 reduced the  
326 levels of most lung inflammatory mediators, the effect was greater in animals boosted with  
327 mRNA-1273.529. Thus, and consistent with the virological data, protection against B.1.1.529-  
328 induced lung inflammation was modestly enhanced in animals boosted with the Omicron-  
329 matched mRNA-1273.529 vaccine.

330

331 **DISCUSSION**

332           Vaccine-induced immunity against SARS-CoV-2 can limit human disease and curtail the  
333 COVID-19 global pandemic. The emergence of SARS-CoV-2 variants with constellations of  
334 amino acid changes in the NTD and RBD of the spike protein jeopardizes vaccines designed  
335 against historical SARS-CoV-2 strains. In the current study, we evaluated in mice the protective  
336 activity of high and low dose formulations of Moderna mRNA-1273 vaccine and matched  
337 (mRNA-1273.529) and non-matched (mRNA-1273) booster doses against the B.1.1.529  
338 Omicron variant. Although the low-dose vaccine arms were designed to model individuals with  
339 suboptimal immune responses, they induce levels of neutralizing antibody in mice comparable  
340 to those measured in human sera after completion of a primary two-dose vaccination series with  
341 mRNA-1273 (Anderson et al., 2020; Widge et al., 2021; Wu et al., 2021). Immunization of mice  
342 with the high-dose formulation of mRNA-1273 induced neutralizing antibodies that inhibited  
343 infection in cell culture of both the historical WA1/2020 D614G and B.1.1.529 viruses, although  
344 we observed reduced efficacy against the Omicron variant, as seen with human sera (Cameroni  
345 et al., 2021; Cao et al., 2021; Dejnirattisai et al., 2022; Liu et al., 2021a). Challenge studies in  
346 K18-hACE2 and 129S2 mice showed robust protection against both SARS-CoV-2 strains with  
347 the high-dose primary series of mRNA-1273 vaccine. In comparison, the neutralizing antibodies  
348 induced by the low-dose series of mRNA-1273 vaccine showed less inhibitory activity against  
349 B.1.1.529, which correlated with breakthrough infection in the upper and lower respiratory tracts.  
350 Analysis of cytokines and histology corroborated the low to minimal protection against B.1.1.529  
351 in K18-hACE2 mice by the low-dose series of mRNA-1273 vaccine.

352           We extended these studies by evaluating the effects of matched and non-matched  
353 mRNA vaccine boosters on antibody responses and protection. In a study with a small cohort of  
354 K18-hACE2 mice, we observed increased serum neutralizing titers one month after boosting  
355 with mRNA-1273, although the response to B.1.1.529 was lower than against WA1/2020. These  
356 data are consistent with data from humans who received a primary mRNA-1273 series and

357 homologous booster; while neutralizing titers were increased against B.1.1.529 after boosting,  
358 levels were lower than against WA1/2020 D614G and waned faster (Pajon et al., 2022).  
359 Because of this pattern, some have advocated for the development of an Omicron variant-  
360 targeted booster to improve protection against infection, disease, and transmission (Waltz,  
361 2022). In our studies in BALB/c mice, as a primary immunization series, an Omicron-targeted  
362 mRNA-1273-529 vaccine robustly induced neutralizing antibodies in serum against B.1.1.529.  
363 However, neutralizing antibody titers against heterologous WA1/2020 D614G, B.1.351, and  
364 B.1.617.2 strains were much lower, as reported by another group (Lee et al., 2022) and also  
365 described in unvaccinated humans that experienced a primary B.1.1.529 infection (Rössler et  
366 al., 2022) . Thus, in unvaccinated, uninfected individuals, bivalent or multivalent mRNA vaccines  
367 (Pajon et al., 2022; Ying et al., 2021) (e.g., mRNA-1273 + mRNA-1273.529) might be required  
368 to achieve necessary breadth of humoral responses.

369         When mRNA-1273.529 was administered as a booster dose after a mRNA-1273 primary  
370 series, we observed enhanced neutralizing responses against B.1.1.529, and this was  
371 associated with protection against B.1.1.529 infection in the upper and lower respiratory tracts.  
372 Moreover, boosting with mRNA-1273.529 also enhanced neutralizing antibody responses  
373 against the historical WA1/2020 D614G strain, albeit less so, which suggests no substantive  
374 detriment in breadth of the mRNA-1273.529 response in the setting of boosting in contrast to  
375 the primary immunization series. Notwithstanding these results, when compared to boosting  
376 with the historical mRNA-1273 vaccine, which increased neutralizing antibody responses  
377 against B.1.1.529 to a lesser degree, the differences in virological protection in the upper and  
378 lower airway were noticeably modest. When mice were given a high-dose mRNA-1273 primary  
379 vaccination series, there was no virological benefit of the Omicron-matched booster compared  
380 to the mRNA-1273 booster, which agrees with recent data from non-human primates (Gagne et  
381 al., 2022). However, when mice given a low-dose primary vaccination series, protection against  
382 lung infection and inflammation was slightly greater in animals boosted with the Omicron-



383 matched mRNA-1273.529 vaccine. The relative disparity between the larger differences in  
384 boosting of neutralizing antibodies by mRNA-1273 and mRNA-1273.529 vaccines and the  
385 smaller effects on infection at one month post-boost could reflect the protective effects of pre-  
386 existing or anamnestic cross-reactive T cells (Gao et al., 2022; Keeton et al., 2022) or Fc  
387 effector function and immune cell engagement by cross-reactive non-neutralizing antibodies  
388 (Bartsch et al., 2021). Further studies examining the durability of protection afforded by mRNA-  
389 1273 versus Omicron-matched mRNA-1273.529 boosters are warranted.

390 **Limitations of study.** We note several limitations in our study. (1) Female K18-hACE2  
391 and 129S2 mice were used to allow for group caging, and some of our studies had smaller  
392 cohorts and were performed in different strains, due to animal availability. Follow-up  
393 experiments in male mice and with larger cohorts are needed to confirm and extend these  
394 results. (2) We used a B.1.1.529 Omicron isolate that lacks an R346K mutation; this substitution  
395 or ones in the emerging BA.2 lineage might further affect vaccine-induced virus neutralization  
396 and protection. (3) Our analysis focused on antibody responses and did not account for possible  
397 cross-reactive T cell responses, which could impact protective immunity. (4) The B.1.1.529 virus  
398 is less pathogenic in mice (Abdelnabi et al., 2021; Bentley et al., 2021; Halfmann et al., 2022).  
399 This could lead to an overestimation of protection compared to other more virulent strains in  
400 mice. (5) We analyzed mRNA-1273 and mRNA-1273.529 booster responses and protection one  
401 month after administration. A time course analysis is needed to assess the durability of the  
402 enhanced neutralizing antibody responses and protection against B.1.1.529. (6) Experiments  
403 were performed exclusively in mice to allow for analysis of multiple arms and comparisons.  
404 Vaccination, boosting, and B.1.1.529 challenge studies in other animal models and ultimately  
405 humans will be required for corroboration.

406 In summary, our studies in mice show protection against B.1.1.529 infection and disease  
407 when mRNA-1273 or Omicron-matched mRNA-1273.529 boosters are administered. While the  
408 low-dose primary immunization series of mRNA-1273 protected against WA1/2020 challenge,

409 we observed substantial loss of serum neutralizing activity against B.1.1.529, and this was  
410 associated with breakthrough infection, inflammation, and disease in the lung after B.1.1.529  
411 challenge. Despite diminished cross-variant neutralization responses by Omicron-matched and  
412 historical mRNA vaccines when administered as primary series immunizations, their delivery as  
413 boosters improved neutralizing responses against B.1.1.529, with slightly better protection  
414 conferred by the matched mRNA-1273.529 booster. Boosting with historical vaccines, variant-  
415 matched mRNA vaccines (Choi et al., 2021; Ying et al., 2021) or possibly heterologous  
416 platforms targeting historical spike proteins (e.g., adenoviral vectored or protein subunit  
417 vaccines (Atmar et al., 2022)) could minimize B.1.1.529 breakthrough infections by increasing  
418 the magnitude of neutralizing anti-SARS-CoV-2 antibodies (Atmar et al., 2021; Munro et al.,  
419 2021) or expanding the breadth of the antibody repertoire to better control variant strains  
420 (Falsey et al., 2021; Naranbhai et al., 2022; Wang et al., 2021). While our data suggest that  
421 certain cohorts (those with lower starting antibody responses) might benefit more from an  
422 Omicron-matched vaccine, further studies evaluating the magnitude and durability of the  
423 boosted immune responses are needed, especially in key vulnerable populations including the  
424 elderly, immunocompromised and immunosuppressed.

425           **Acknowledgements.** This study was supported by the NIH (R01 AI157155, NIAID  
426 Centers of Excellence for Influenza Research and Response (CEIRR) contracts  
427 HHSN272201400008C, 75N93021C00014, and 75N93019C00051). We thank Marciela  
428 DeGrace for help in study design and funding support, Pei-Yong Shi for the WA1/2020 strains,  
429 and Peter Halfmann and Yoshihiro Kawaoka for the B.1.1.529 isolate used in this study. We  
430 also acknowledge the Pulmonary Morphology Core at Washington University School of  
431 Medicine for tissue sectioning and slide imaging, and thank Michael Whitt for support on VSV-  
432 based pseudovirus production.

433           **Author contributions.** B.Y. and S.M.S. performed and analyzed live virus neutralization  
434 assays. B.Y., S.M.S., B.W., C.Y.L., O.K., S.M., Z.C. and J.B.T. performed mouse experiments.  
435 B.W. and B.Y. performed and analyzed viral burden analyses. B.Y., L.M., T.K., C.S., and A.W.  
436 performed ELISA binding experiments and analysis. K.W., D.L., D.M.B., and L.E.A. performed  
437 pseudovirus neutralization assays and analysis. A.C., S.E. and D.K.E. provided mRNA vaccines  
438 and helped design experiments. L.B.T. and M.S.D. designed studies and supervised the  
439 research. M.S.D. and L.B.T. wrote the initial draft, with the other authors providing editorial  
440 comments.

441           **Competing interests.** M.S.D. is a consultant for Inbios, Vir Biotechnology, Senda  
442 Biosciences, and Carnival Corporation, and on the Scientific Advisory Boards of Moderna and  
443 Immunome. The Diamond laboratory has received unrelated funding support in sponsored  
444 research agreements from Vir Biotechnology, Kaleido, and Emergent BioSolutions and past  
445 support from Moderna not related to these studies. K.W., D.L., L.E.A., L.M., T.K., C.S., A.W.,  
446 A.C., S.E. and D.K.E. are employees of and shareholders in Moderna Inc.

447 **FIGURE LEGENDS**

448 **Figure 1. Antibody responses of mRNA vaccines in K18-hACE2 mice.** Seven-week-  
449 old female K18-hACE2 transgenic mice were immunized with 5 or 0.1  $\mu\text{g}$  of mRNA vaccines. **A.**  
450 Scheme of immunizations, blood draw, and virus challenge. **B.** Binding of sarbecovirus cross-  
451 reactive monoclonal antibodies to Wuhan-1 and B.1.1.529 spike and RBD proteins. **C-F.** Serum  
452 IgG responses at three weeks after the second 5  $\mu\text{g}$  (**C-D**) or 0.1  $\mu\text{g}$  (**E-F**) dose of mRNA  
453 vaccines (control or mRNA-1273) against indicated spike (**C, E**) or RBD (**D, F**) proteins ( $n = 12$ ,  
454 two experiments, boxes illustrate geometric mean values, dotted lines show the limit of  
455 detection (LOD)). **G.** Serum neutralizing antibody responses three weeks after second vaccine  
456 dose as judged by focus reduction neutralization test (FRNT) with WA1/2020 D614G (*left panel*)  
457 and B.1.1.529 (*right panel*) in mice immunized with 5 or 0.1  $\mu\text{g}$  of control ( $n = 4$ ) or mRNA-1273  
458 ( $n = 12$ ) vaccines (two experiments, boxes illustrate geometric mean titer (GMT) values, dotted  
459 lines show the LOD). **H.** Paired analysis of serum neutralizing titers against WA1/2020 D614G  
460 and B.1.1.529 from individual mice (data from **G**) from samples obtained three weeks after the  
461 second 5  $\mu\text{g}$  (*left panel*) or 0.1  $\mu\text{g}$  (*right panel*) dose of mRNA-1273 ( $n = 12$ , two experiments,  
462 dotted lines show the LOD). GMT values are indicated at the top of the graphs. Statistical  
463 analyses. **C-F:** Mann-Whitney test; **G:** One-way ANOVA with Dunn's post-test; **H:** Wilcoxon  
464 signed-rank test (\*\*  $P < 0.01$ ; \*\*\*  $P < 0.001$ ; \*\*\*\*  $P < 0.0001$ ).

465 **Figure 2. Protection against SARS-CoV-2 infection after mRNA vaccination in K18-**  
466 **hACE2 mice.** Seven-week-old female K18-hACE2 transgenic mice were immunized with 5 or  
467 0.1  $\mu\text{g}$  of mRNA vaccines as described in **Fig 1A**. Five weeks after completing a primary  
468 vaccination series, mice were challenged with  $10^4$  focus-forming units (FFU) of WA1/2020  
469 D614G or B.1.1.529. **A-B.** Body weight change in animals immunized with 5  $\mu\text{g}$  (**A**) or 0.1  $\mu\text{g}$   
470 (**B**) of control or mRNA-1273 vaccines between days 0 and 6 after challenge with WA1/2020  
471 D614G or B.1.1.529. Data show mean values ( $n = 7-8$ , two experiments). **C-H.** Viral burden at 6

472 dpi in the nasal washes (**C, F**), nasal turbinates (**D, G**), and lungs (**E, H**) as assessed by qRT-  
473 PCR of the *N* gene after WA1/2020 D614G or B.1.1.529 challenge of mice immunized with 5  $\mu$ g  
474 (**C-E**) or 0.1  $\mu$ g (**F-H**) of control or mRNA-1273 vaccines (n = 7-8, two experiments, boxes  
475 illustrate median values, dotted lines show LOD). Statistical analyses: **A-B**, unpaired t test; **C-H**:  
476 Mann-Whitney test (ns, not significant; \*  $P < 0.05$ ; \*\*  $P < 0.01$ ; \*\*\*  $P < 0.001$ ; \*\*\*\*  $P < 0.0001$ ). **I**.  
477 Correlation analyses comparing serum neutralizing antibody concentrations three weeks after  
478 the second vaccine dose and lung viral titers (6 dpi) in K18-hACE2 mice after challenge with  
479 WA1/2020 D614G (*left panel*) or B.1.1.529 (*right panel*); Pearson's correlation  $R^2$  and  $P$  values  
480 are indicated as insets; closed symbols 5  $\mu$ g vaccine dose; open symbols, 0.1  $\mu$ g vaccine dose.

481 **Figure 3. mRNA vaccine protection against disease in K18-hACE2 transgenic**  
482 **mice.** Seven-week-old female K18-hACE2 transgenic mice were immunized with two 5 or 0.1  
483  $\mu$ g doses of mRNA vaccines, and challenged with WA1/2020 D614G or B.1.1.529. as described  
484 in **Fig 1 and 2. A-B.** Heat-maps of cytokine and chemokine levels in lung homogenates at 6 dpi  
485 in animals immunized with 5  $\mu$ g (**A**) or 1  $\mu$ g (**B**) doses of indicated mRNA vaccines. Fold-change  
486 was calculated relative to naive uninfected mice, and  $\log_2$  values are plotted (2 experiments, n =  
487 7-8 per group except naive, n = 4). The full data set is shown in **Table S1-S2. C-E.** Hematoxylin  
488 and eosin staining of lung sections harvested from control or mRNA-1273 vaccinated animals (5  
489  $\mu$ g dose, **C**; 1  $\mu$ g dose, **D**) at 6 dpi with WA1/2020 D614G or B.1.1.529. A section from an  
490 uninfected animal (**E**) is shown for comparison. Images show low- (left; scale bars, 1 mm),  
491 moderate- (middle, scale bars, 200  $\mu$ m), and high-power (bottom; scale bars, 50  $\mu$ m).  
492 Representative images of multiple lung sections from n = 3 per group.

493 **Figure 4. A booster dose of mRNA-1273 enhances neutralizing antibody**  
494 **responses and confers protection in K18-hACE2 mice.** Seven-week-old female K18-hACE2  
495 transgenic mice were immunized with 5 or 0.25  $\mu$ g of mRNA vaccines and boosted 17 to 19  
496 weeks later with 1  $\mu$ g of mRNA-1273. **A.** Scheme of immunizations, blood draws, and virus

497 challenge. **B-C**. Serum neutralizing antibody responses immediately before (**B**, pre-boost) and  
498 four weeks after (**C**, post-boost) a control or mRNA-1273 booster dose as judged by FRNT with  
499 WA1/2020 D614G (*left panel*) and B.1.1.529 (*right panel*) in mice immunized with 5 or 0.25  $\mu\text{g}$   
500 of control (n = 4) or mRNA-1273 (5  $\mu\text{g}$ , n = 8; 0.25  $\mu\text{g}$ , n = 4) vaccines (one experiment, boxes  
501 illustrate geometric mean titer (GMT) values, dotted lines show the LOD). **D-E**. Paired analysis  
502 of pre-boost (**D**) and post-boost (**E**) serum neutralizing titers against WA1/2020 D614G and  
503 B.1.1.529 from individual mice (data from **B-C**) from samples obtained from animals that  
504 received a primary 5  $\mu\text{g}$  (*left panel*) or 0.25  $\mu\text{g}$  (*right panel*) dose series of mRNA-1273 vaccine  
505 (n = 4 to 8, one experiment, dotted lines show the LOD). GMT values are indicated at the top of  
506 the graphs. **F-G**. Four weeks after boosting with control or mRNA-1273, K18-hACE2 mice were  
507 challenged with  $10^4$  FFU of B.1.1.529. Viral burden at 6 dpi in the nasal washes, nasal  
508 turbinates, and lungs as assessed by *N* gene levels in animals that had received a primary  
509 series immunization with 5  $\mu\text{g}$  (**F**) or 0.25  $\mu\text{g}$  (**G**) doses of control or mRNA-1273 vaccines (n =  
510 7-8, two experiments, boxes illustrate median values, dotted lines show LOD). Statistical  
511 analyses. **D-E**. Wilcoxon signed-rank test; **F-G**: Mann-Whitney test (ns, not significant; \*\*  $P <$   
512 0.01; \*\*\*  $P <$  0.001).

513 **Figure 5. Antibody responses in BALB/c mice after immunization with mRNA-1273**  
514 **and mRNA-1273.529 vaccines.** Six-to-eight-week-old female BALB/c mice were immunized  
515 twice over a three-week interval with 1  $\mu\text{g}$  of mRNA-1273 or mRNA-1273.529 vaccine or a PBS  
516 control (black circles). Immediately before (Day 21) or two weeks after (Day 36) the second  
517 vaccine dose, serum was collected. **A**. Scheme of immunization and blood draws. **B**. Serum  
518 antibody binding to Wuhan-1 or B.1.1.529 spike proteins by ELISA (n = 8, two experiments,  
519 boxes illustrate mean values, dotted lines show the LOD). **C**. Neutralizing activity of serum  
520 obtained two weeks after (Day 36) immunization with mRNA-1273 or mRNA-1273.529 vaccine  
521 against VSV pseudoviruses displaying the spike proteins of Wuhan-1 D614G, B.1.351 (Beta),

522 B.1.617.2 (Delta), or B.1.1.529 (Omicron) ( $n = 8$ , two experiments, boxes illustrate geometric  
523 mean values, dotted lines show the LOD). GMT values are indicated above the columns.

524 **Figure 6. Booster doses of mRNA-1273 or mRNA-1273.529 enhance neutralizing**  
525 **antibody responses in 129S2 mice.** Seven-week-old female 129S2 mice were immunized with  
526 5 or 0.25  $\mu\text{g}$  of mRNA vaccines and then boosted 10 to 11 weeks later with 1  $\mu\text{g}$  of control  
527 mRNA, mRNA-1273, or mRNA-1273.529. **A.** Scheme of immunizations, blood draws, and virus  
528 challenge. **B-C.** Serum neutralizing antibody responses immediately before (**B**, pre-boost) and  
529 three to four weeks after (**C**, post-boost) a control, mRNA-1273, or mRNA-1273.529 booster  
530 dose as judged by FRNT with WA1/2020 N501Y/D614G (*left panel(s)*) and B.1.1.529 (*right*  
531 *panel(s)*) in 129S2 mice that received primary series immunizations with 5 or 0.25  $\mu\text{g}$  of control  
532 ( $n = 6$ ) or mRNA-1273 ( $n = 30$ ) vaccines (two experiments, boxes illustrate geometric mean  
533 values, dotted lines show the LOD). **D-E.** Paired analysis of pre- and post-boost serum  
534 neutralizing titers against WA1/2020 D614G (**D**) and B.1.1.529 (**E**) viruses from samples  
535 obtained from animals (data from **B-C**) that received the following primary and booster  
536 immunizations: mRNA-1273 (5 or 0.25  $\mu\text{g}$ ) + control booster, mRNA-1273 (5 or 0.25  $\mu\text{g}$ ) +  
537 mRNA-1273 booster, mRNA-1273 (5 or 0.25  $\mu\text{g}$ ) + mRNA-1273.529 booster ( $n = 10$ , two  
538 experiments, dotted lines show the LOD). GMT values are indicated at the top of the graphs.  
539 Statistical analyses. **B-C:** One-way ANOVA with Dunn's post-test; **D-E.** Wilcoxon signed-rank  
540 test (ns, not significant; \*  $P < 0.05$ ; \*\*  $P < 0.01$ ; \*\*\*  $P < 0.001$ ; \*\*\*\*  $P < 0.0001$ ).

541 **Figure 7. Booster doses of mRNA-1273 or mRNA-1273.529 enhance protection**  
542 **against B.1.1.529 infection in 129S2 mice.** Seven-week-old female 129S2 mice were  
543 immunized with 5 or 0.25  $\mu\text{g}$  of mRNA vaccines, boosted with 1  $\mu\text{g}$  of control mRNA, mRNA-  
544 1273, or mRNA-1273.529 and challenged with WA1/2020 N501Y/D614G or B.1.1.529, as  
545 described in **Fig 6**. **A-B.** Viral RNA levels at 3 dpi in the nasal washes, nasal turbinates, and  
546 lungs after WA1/2020 N501Y/D614G or B.1.1.529 challenge of mice immunized with 5  $\mu\text{g}$  (**A**) or

547 0.25  $\mu$ g (**B**) of control or mRNA-1273 vaccines and boosted with control, mRNA-1273, or  
548 mRNA-1273.529 vaccine (n = 8-10 per group, two experiments, boxes illustrate mean values,  
549 dotted lines show LOD; One-way ANOVA with Tukey's post-test: ns, not significant; \*  $P < 0.05$ ;  
550 \*\*  $P < 0.01$ ; \*\*\*  $P < 0.001$ ; \*\*\*\*  $P < 0.0001$ ). **C-D**. Heat-maps of cytokine and chemokine levels in  
551 lung homogenates at 3 dpi with WA1/2020 N501Y/D614G or B.1.1.529 in animals immunized  
552 with 5  $\mu$ g (**C**) or 0.25  $\mu$ g (**D**) doses of control or mRNA-1273 vaccines and then boosted with  
553 control, mRNA-1273, or mRNA-1273.529 vaccines. Fold-change was calculated relative to  
554 naive mice, and  $\log_2$  values are plotted (2 experiments, n = 8 per group except naive, n = 4).  
555 The full data set is shown in **Table S3-S4**.

556

#### 557 **SUPPLEMENTAL FIGURE LEGENDS**

558 **Figure S1. Serum neutralization of WA1/2020 D614G and B.1.1.529, Related to Fig**  
559 **1.** Seven-week-old female K18-hACE2 transgenic mice were immunized with 5 or 0.1  $\mu$ g of  
560 mRNA vaccines. Serum neutralizing antibody responses against WA1/2020 D614G and  
561 B.1.1.529 were assessed three weeks after the second vaccine dose (control mRNA, *top*;  
562 mRNA-1273, *bottom*) from mice immunized with 5 or 0.1  $\mu$ g of control (n = 4) or mRNA-1273 (n  
563 = 12) vaccines. Neutralization curves corresponding to individual mice are shown for the  
564 indicated vaccines. Each point represents the mean of two technical replicates.

565 **Figure S2. Serum neutralization of WA1/2020 D614G and B.1.1.529, Related to Fig**  
566 **4.** Seven-week-old female K18-hACE2 transgenic mice were immunized with 5 or 0.25  $\mu$ g of  
567 mRNA vaccines and then boosted approximately 17 to 19 weeks later with 1  $\mu$ g of mRNA-1273.  
568 Serum neutralizing antibody responses against WA1/2020 D614G and B.1.1.529 immediately  
569 before (**A**, pre-boost) and four weeks after (**B**, post-boost) a control or mRNA-1273 booster  
570 dose from mice immunized with 5 or 0.25  $\mu$ g of control (n = 4) or mRNA-1273 (5  $\mu$ g, n = 8; 0.25



571  $\mu\text{g}$ ,  $n = 4$ ) vaccines. Neutralization curves corresponding to individual mice are shown for the  
572 indicated immunizations. Each point represents the mean of two technical replicates.

573 **Figure S3. Pre- and post-boost serum neutralization of WA1/2020 N501Y/D614G**  
574 **and B.1.1.529, Related to Fig 6.** Seven-week-old female 129S2 mice were immunized with 5  
575 or 0.25  $\mu\text{g}$  of mRNA vaccines and then boosted 10 to 11 weeks later with 1  $\mu\text{g}$  of control mRNA,  
576 mRNA-1273, or mRNA-1273.529. Neutralizing antibody responses against WA1/2020  
577 N501Y/D614G and B.1.1.529 from serum immediately before (top) or one month after boosting  
578 (bottom) with indicated vaccines from 129S2 mice that had received primary series  
579 immunizations with 5 or 0.25  $\mu\text{g}$  of control or mRNA-1273 vaccines. Neutralization curves  
580 corresponding to individual mice are shown for the indicated immunizations. Serum are from  
581 two independent experiments, and each point from a neutralization curve represents the mean  
582 of two technical replicates.

583

#### 584 **SUPPLEMENTAL TABLE TITLES**

585 **Supplemental Table S1. Cytokine and chemokine concentrations in K18-hACE2**  
586 **mice vaccinated with two 5  $\mu\text{g}$  doses of mRNA vaccines and challenged with WA1/2020**  
587 **D614G or B.1.1.529, Related to Fig 3.**

588 **Supplemental Table S2: Cytokine and chemokine concentrations in K18-hACE2**  
589 **mice vaccinated with two 0.1  $\mu\text{g}$  doses of mRNA vaccines and challenged with WA1/2020**  
590 **D614G or B.1.1.529, Related to Fig 3.**

591 **Supplemental Table S3: Cytokine and chemokine concentrations in 129S2 mice**  
592 **immunized with 5  $\mu\text{g}$  primary series and 1  $\mu\text{g}$  booster dose and challenged with**  
593 **WA1/2020 N501Y/D614G or B.1.1.529, Related to Fig 7.**

594 **Supplemental Table S4: Cytokine and chemokine concentrations in 129S2 mice**  
595 **immunized with 0.25 µg primary series and 1 µg booster dose and challenged with**  
596 **WA1/2020 N501Y/D614G or B.1.1.529, Related to Fig 7.**

597 **STAR METHODS**

598 **RESOURCE AVAILABILITY**

599 **Lead contact.** Further information and requests for resources and reagents should be  
600 directed to the Lead Contact, Michael S. Diamond ([mdiamond@wustl.edu](mailto:mdiamond@wustl.edu)).

601 **Materials availability.** All requests for resources and reagents should be directed to the  
602 Lead Contact author. This includes viruses, vaccines, and primer-probe sets. All reagents will  
603 be made available on request after completion of a Materials Transfer Agreement (MTA). The  
604 mRNA vaccines (control, mRNA-1273, and mRNA-1273.529) can be obtained under an MTA  
605 with Moderna (contact: Darin Edwards, [Darin.Edwards@modernatx.com](mailto:Darin.Edwards@modernatx.com)).

606 **Data and code availability.** All data supporting the findings of this study are available  
607 within the paper and are available from the corresponding author upon request. This paper does  
608 not include original code. Any additional information required to reanalyze the data reported in  
609 this paper is available from the lead contact upon request.

610

611 **EXPERIMENTAL MODEL AND SUBJECT DETAILS**

612 **Cells.** African green monkey Vero-TMPRSS2 (Zang et al., 2020) and Vero-hACE2-  
613 TMPRSS2 (Chen et al., 2021c) cells were cultured at 37°C in Dulbecco's Modified Eagle  
614 medium (DMEM) supplemented with 10% fetal bovine serum (FBS), 10 mM HEPES pH 7.3,  
615 1 mM sodium pyruvate, 1× non-essential amino acids, and 100 U/mL of penicillin-  
616 streptomycin. Vero-TMPRSS2 cells were supplemented with 5 µg/mL of blasticidin. Vero-  
617 hACE2-TMPRSS2 cells were supplemented with 10 µg/mL of puromycin. All cells routinely  
618 tested negative for mycoplasma using a PCR-based assay.

619           **Viruses.** The WA1/2020 recombinant strain with D614G substitution was described  
620 previously (Plante et al., 2020). The B.1.1.529 isolate (hCoV-19/USA/WI-WSLH-221686/2021)  
621 was obtained from an individual in Wisconsin as a midturbinate nasal swab and passaged once  
622 on Vero-TMPRSS2 cells (Imai et al., 2020). All viruses were subjected to next-generation  
623 sequencing (Chen et al., 2021c) to confirm the introduction and stability of substitutions. All virus  
624 experiments were performed in an approved biosafety level 3 (BSL-3) facility.

625           **Mice.** Animal studies were carried out in accordance with the recommendations in the  
626 Guide for the Care and Use of Laboratory Animals of the National Institutes of Health. For  
627 studies (K18-hACE2 and 129S2 mice) at Washington University School of Medicine, the  
628 protocols were approved by the Institutional Animal Care and Use Committee at the Washington  
629 University School of Medicine (assurance number A3381-01). Virus inoculations were  
630 performed under anesthesia that was induced and maintained with ketamine hydrochloride and  
631 xylazine, and all efforts were made to minimize animal suffering. For studies with BALB/c mice,  
632 animal experiments were carried out in compliance with approval from the Animal Care and Use  
633 Committee of Moderna, Inc. Sample size for animal experiments was determined on the basis  
634 of criteria set by the institutional Animal Care and Use Committee. Experiments were neither  
635 randomized nor blinded.

636           Heterozygous K18-hACE2 C57BL/6J mice (strain: 2B6.Cg-Tg(K18-ACE2)2Prlmn/J, Cat  
637 # 34860) were obtained from The Jackson Laboratory. 129S2 mice (strain: 129S2/SvPasCrl,  
638 Cat # 287) and BALB/c mice (strain: BALB/cAnNCrl, Cat # 028) were obtained from Charles  
639 River Laboratories. Animals were housed in groups and fed standard chow diets.

640

## 641 **METHOD DETAILS**

642           **Pre-clinical vaccine mRNA and lipid nanoparticle production process.** A sequence-  
643 optimized mRNA encoding prefusion-stabilized Wuhan-Hu-1 (mRNA-1273) SARS-CoV-2 S-2P  
644 or B.1.1.529 (mRNA-1273.529) protein was synthesized *in vitro* using an optimized T7 RNA

645 polymerase-mediated transcription reaction with complete replacement of uridine by N1m-  
646 pseudouridine (Nelson et al., 2020). The pre-clinical mRNA-1273.529 vaccine encoded the  
647 following substitutions: A67V,  $\Delta$ 69-70, T95I, G142D,  $\Delta$ 143-145,  $\Delta$ 211, L212I, ins214EPE,  
648 G339D, S371L, S373P, S375F, K417N, N440K, G446S, S477N, T478K, E484A, Q493K,  
649 G496S, Q498R, N501Y, Y505H, T547K, D614G, H655Y, N679K, P681H, N764K, D796Y,  
650 N856K, Q954H, N969K, and L981F. A non-translating control mRNA was synthesized and  
651 formulated into lipid nanoparticles as previously described (Corbett et al., 2020). The reaction  
652 included a DNA template containing the immunogen open-reading frame flanked by 5'  
653 untranslated region (UTR) and 3' UTR sequences, and was terminated by an encoded polyA  
654 tail. After RNA transcription, the cap-1 structure was added using the vaccinia virus capping  
655 enzyme and 2'-O-methyltransferase (New England Biolabs). The mRNA was purified by oligo-  
656 dT affinity purification, buffer exchanged by tangential flow filtration into sodium acetate, pH 5.0,  
657 sterile filtered, and kept frozen at  $-20^{\circ}\text{C}$  until further use.

658 The mRNA was encapsulated in a lipid nanoparticle through a modified ethanol-drop  
659 nanoprecipitation process described previously (Hassett et al., 2019). Ionizable, structural,  
660 helper, and polyethylene glycol lipids were briefly mixed with mRNA in an acetate buffer, pH 5.0,  
661 at a ratio of 2.5:1 (lipid:mRNA). The mixture was neutralized with Tris-HCl, pH 7.5, sucrose was  
662 added as a cryoprotectant, and the final solution was sterile-filtered. Vials were filled with  
663 formulated lipid nanoparticle and stored frozen at  $-20^{\circ}\text{C}$  until further use. The pre-clinical  
664 vaccine product underwent analytical characterization, which included the determination of  
665 particle size and polydispersity, encapsulation, mRNA purity, double-stranded RNA content,  
666 osmolality, pH, endotoxin, and bioburden, and the material was deemed acceptable for *in*  
667 *vivo* study.

668 **Viral antigens.** Recombinant soluble S and RBD proteins from Wuhan-1 and B.1.1.529  
669 SARS-CoV-2 strains were expressed as described (Amanat et al., 2021; Stadlbauer et al.,  
670 2020). Recombinant proteins were produced in Expi293F cells (ThermoFisher) by transfection

671 of DNA using the ExpiFectamine 293 Transfection Kit (ThermoFisher). Supernatants were  
672 harvested 3 days post-transfection, and recombinant proteins were purified using Ni-NTA  
673 agarose (ThermoFisher), then buffer exchanged into PBS and concentrated using Amicon  
674 Ultracel centrifugal filters (EMD Millipore).

675 **ELISA.** Assays were performed in 96-well microtiter plates (Thermo Fisher) coated with  
676 50  $\mu$ L of recombinant Wuhan-1 or B.1.1.529 spike or RBD proteins. Plates were incubated at  
677 4°C overnight and then blocked with 200  $\mu$ L of 3% non-fat dry milk (AmericanBio) in PBS  
678 containing 0.1% Tween-20 (PBST) for 1 h at room temperature (RT). Sera were serially diluted  
679 in 1% non-fat dry milk in PBST and added to the plates. Plates were incubated for 2 h at room  
680 temperature and then washed 3 times with PBST. Goat anti-mouse IgG-HRP (Sigma-Aldrich,  
681 1:9000) was diluted in 1% non-fat dry milk in PBST before adding to the wells and incubating for  
682 1 h at room temperature. Plates were washed 3 times with PBST before the addition of  
683 peroxidase substrate (SigmaFAST o-phenylenediamine dihydrochloride, Sigma-Aldrich).  
684 Reactions were stopped by the addition of 3 M hydrochloric acid. Optical density (OD)  
685 measurements were taken at 490 nm, and endpoint titers were calculated in excel using a 0.15  
686 OD 490 nm cutoff. Graphs were generated using Graphpad Prism v9.

687 **Focus reduction neutralization test.** Serial dilutions of sera were incubated with  $10^2$   
688 focus-forming units (FFU) of WA1/2020 D614G or B.1.1.529 for 1 h at 37°C. Antibody-virus  
689 complexes were added to Vero-TMPRSS2 cell monolayers in 96-well plates and incubated at  
690 37°C for 1 h. Subsequently, cells were overlaid with 1% (w/v) methylcellulose in MEM. Plates  
691 were harvested 30 h later by removing overlays and fixed with 4% PFA in PBS for 20 min at  
692 room temperature. Plates were washed and sequentially incubated with an oligoclonal pool of  
693 SARS2-2, SARS2-11, SARS2-16, SARS2-31, SARS2-38, SARS2-57, and SARS2-71(Liu et al.,  
694 2021c) anti-S antibodies and HRP-conjugated goat anti-mouse IgG (Sigma Cat # A8924, RRID:  
695 AB\_258426) in PBS supplemented with 0.1% saponin and 0.1% bovine serum albumin. SARS-

696 CoV-2-infected cell foci were visualized using TrueBlue peroxidase substrate (KPL) and  
697 quantitated on an ImmunoSpot microanalyzer (Cellular Technologies).

698 **Pseudovirus neutralization assay.** Codon-optimized full-length spike genes (Wuhan-1  
699 with D614G, B.1.351, B.1.617.2, and B.1.1.529) were cloned into a pCAGGS vector. Spike  
700 genes of contained the following mutations: B.1.351: L18F-D80A-D215G-L242-244del-R246I-  
701 K417N-E484K-N501Y-D614G-A701V; B.1.617.2: T19R-T95I-G142D-E156G-F157del-R158del-  
702 L452R-T478K-D614G-P681R-D950N; and B.1.1.529: A67V,  $\Delta$ 69-70, T95I, G142D/ $\Delta$ VYY143-  
703 145,  $\Delta$ N211/L212I, ins214EPE, G339D, S371L, S373P, S375F, K417N, N440K, G446S,  
704 S477N, T478K, E484A, Q493R, G496S, Q498R, N501Y, Y505H, T547K, D614G, H655Y,  
705 N679K, P681H, N764K, D796Y, N856K, Q954H, N969K, L981F. To generate VSV $\Delta$ G-based  
706 SARS-CoV-2 pseudovirus, BHK-21/WI-2 cells were transfected with the spike expression  
707 plasmid and infected by VSV $\Delta$ G-firefly-luciferase as previously described (Whitt, 2010). A549-  
708 hACE2-TMPRSS2 cells were used as target cells for the neutralization assay and maintained in  
709 DMEM supplemented with 10% fetal bovine serum and 1  $\mu$ g/mL puromycin. To perform  
710 neutralization assay, mouse serum samples were heat-inactivated for 45 min at 56°C, and serial  
711 dilutions were made in DMEM supplemented with 10% FBS. The diluted serum samples or  
712 culture medium (serving as virus only control) were mixed with VSV $\Delta$ G-based SARS-CoV-2  
713 pseudovirus and incubated at 37°C for 45 min. The inoculum virus or virus-serum mix was  
714 subsequently used to infect A549-hACE2-TMPRSS2 cells for 18 h at 37°C. At 18 h post  
715 infection, an equal volume of One-Glo reagent (Promega; E6120) was added to culture medium  
716 for readout using BMG PHERastar-FS plate reader. The percentage of neutralization was  
717 calculated based on relative light units of the virus control, and subsequently analyzed using  
718 four parameter logistic curve (Prism 8,0).

719 **Mouse experiments.** (a) K18hACE2 transgenic mice. Seven-week-old female K18-  
720 hACE2 C57BL/6 mice were immunized three weeks apart with 5, 0.25, or 0.1  $\mu$ g of mRNA  
721 vaccines (control or mRNA-1273) in 50  $\mu$ l of PBS via intramuscular injection in the hind leg.

722 Animals were bled three to four weeks after the second vaccine dose for immunogenicity  
723 analysis. In some experiments, four weeks after completing the primary series immunization,  
724 mice were challenged with  $10^4$  FFU of WA1/2020 D614G or B.1.1.529 of SARS-CoV-2 strains  
725 by the intranasal route. In other experiments, 17 to 19 weeks after completing the primary series  
726 immunization, animals were bled for antibody analysis, and then boosted with 1  $\mu$ g of control or  
727 mRNA-1273 vaccine. Four weeks later, K18-hACE2 mice were challenged with  $10^4$  FFU of  
728 B.1.1.529 by the intranasal route. For some studies, weights were measured at day 0 and 6,  
729 and in all experiments, animals were euthanized at 6 dpi. Tissues were harvested for virological,  
730 immunological, and pathological analyses.

731 (b) BALB/c mice. 6 to 8-week-old female BALB/c mice were immunized three weeks  
732 apart with 1 or 0.1  $\mu$ g of mRNA vaccines (mRNA-1273 or mRNA-1273.529) or PBS (in 50  $\mu$ L)  
733 via intramuscular injection in the quadriceps muscle of the hind leg under isoflurane anesthesia.  
734 Blood was sampled three weeks after the first immunization and two weeks after the second  
735 immunization, and anti-spike and neutralizing antibody levels were measured by ELISA and a  
736 VSV-based pseudovirus neutralization assay.

737 (c) 129S2 mice. Seven-week-old female 129S2 mice were immunized three weeks apart  
738 with 5 or 0.25  $\mu$ g of mRNA vaccines (control, mRNA-1273) in 50  $\mu$ l of PBS via intramuscular  
739 injection in the hind leg. Ten to eleven weeks later, animals were bled (pre-boost), and  
740 subsequently boosted with 1  $\mu$ g of control, mRNA-1273, or mRNA-1273.529 vaccine. Three to  
741 four weeks later, animals were bled again (pos-boost), and then challenged with  $10^4$  FFU of  
742 B.1.1.529 by the intranasal route. Animals were euthanized at 3 dpi, and tissues were harvested  
743 for virological and cytokine/chemokine analyses.

744 **Measurement of viral burden.** Tissues were weighed and homogenized with zirconia  
745 beads in a MagNA Lyser instrument (Roche Life Science) in 1 ml of DMEM medium  
746 supplemented with 2% heat-inactivated FBS. Tissue homogenates were clarified by

747 centrifugation at 10,000 rpm for 5 min and stored at  $-80^{\circ}\text{C}$ . RNA was extracted using the  
748 MagMax mirVana Total RNA isolation kit (Thermo Fisher Scientific) on the Kingfisher Flex  
749 extraction robot (Thermo Fisher Scientific). RNA was reverse transcribed and amplified using  
750 the TaqMan RNA-to-CT 1-Step Kit (Thermo Fisher Scientific). Reverse transcription was carried  
751 out at  $48^{\circ}\text{C}$  for 15 min followed by 2 min at  $95^{\circ}\text{C}$ . Amplification was accomplished over 50  
752 cycles as follows:  $95^{\circ}\text{C}$  for 15 s and  $60^{\circ}\text{C}$  for 1 min. Copies of SARS-CoV-2 *N* gene RNA in  
753 samples were determined using a published assay (Case et al., 2020a).

754 **Cytokine and chemokine protein measurements.** Lung homogenates were incubated  
755 with Triton-X-100 (1% final concentration) for 1 h at room temperature to inactivate SARS-CoV-  
756 2. Homogenates were analyzed for cytokines and chemokines by Eve Technologies  
757 Corporation (Calgary, AB, Canada) using their Mouse Cytokine Array/Chemokine Array 31-Plex  
758 (MD31) platform.

759 **Lung histology.** Lungs of euthanized mice were inflated with  $\sim 2$  mL of 10% neutral  
760 buffered formalin using a 3-mL syringe and catheter inserted into the trachea and kept in fixative  
761 for 7 days. Tissues were embedded in paraffin, and sections were stained with hematoxylin and  
762 eosin. Images were captured using the Nanozoomer (Hamamatsu) at the Alafi Neuroimaging  
763 Core at Washington University.

764

## 765 **QUANTIFICATION AND STATISTICAL ANALYSES**

766 Statistical significance was assigned when *P* values were  $< 0.05$  using GraphPad Prism  
767 version 9.3. Tests, number of animals, median values, and statistical comparison groups are  
768 indicated in the Figure legends. Changes in infectious virus titer, viral RNA levels, or serum  
769 antibody responses were compared to unvaccinated or mRNA-control immunized animals and  
770 were analyzed by one-way ANOVA with a multiple comparisons correction, Mann-Whitney test,



771 or Wilcoxon signed-rank test depending on the type of results, number of comparisons, and  
772 distribution of the data.

773 **REFERENCES**

- 774 Abdelnabi, R., Foo, C.S., Zhang, X., Lemmens, V., Maes, P., Slechten, B., Raymenants, J.,  
775 André, E., Weynand, B., Dallemier, K., *et al.* (2021). The omicron (B.1.1.529) SARS-CoV-2  
776 variant of concern does not readily infect Syrian hamsters. *bioRxiv*, 2021.2012.2024.474086.  
777
- 778 Amanat, F., Thapa, M., Lei, T., Ahmed, S.M.S., Adelsberg, D.C., Carreño, J.M., Strohmeier, S.,  
779 Schmitz, A.J., Zafar, S., Zhou, J.Q., *et al.* (2021). SARS-CoV-2 mRNA vaccination induces  
780 functionally diverse antibodies to NTD, RBD, and S2. *Cell* *184*, 3936-3948.e3910.  
781
- 782 Anderson, E.J., Roupahel, N.G., Widge, A.T., Jackson, L.A., Roberts, P.C., Makhene, M.,  
783 Chappell, J.D., Denison, M.R., Stevens, L.J., Puijssers, A.J., *et al.* (2020). Safety and  
784 Immunogenicity of SARS-CoV-2 mRNA-1273 Vaccine in Older Adults. *N Engl J Med* *383*, 2427-  
785 2438.  
786
- 787 Atmar, R.L., Lyke, K.E., Deming, M.E., Jackson, L.A., Branche, A.R., El Sahly, H.M., Rostad,  
788 C.A., Martin, J.M., Johnston, C., Rupp, R.E., *et al.* (2021). Heterologous SARS-CoV-2 Booster  
789 Vaccinations - Preliminary Report. *medRxiv : the preprint server for health sciences*.  
790
- 791 Atmar, R.L., Lyke, K.E., Deming, M.E., Jackson, L.A., Branche, A.R., El Sahly, H.M., Rostad,  
792 C.A., Martin, J.M., Johnston, C., Rupp, R.E., *et al.* (2022). Homologous and Heterologous  
793 Covid-19 Booster Vaccinations. *N Engl J Med*.  
794
- 795 Bar-On, Y.M., Goldberg, Y., Mandel, M., Bodenheimer, O., Freedman, L., Kalkstein, N., Mizrahi,  
796 B., Alroy-Preis, S., Ash, N., Milo, R., *et al.* (2021). Protection of BNT162b2 Vaccine Booster  
797 against Covid-19 in Israel. *N Engl J Med* *385*, 1393-1400.  
798
- 799 Barnes, C.O., Jette, C.A., Abernathy, M.E., Dam, K.A., Esswein, S.R., Gristick, H.B., Malyutin,  
800 A.G., Sharaf, N.G., Huey-Tubman, K.E., Lee, Y.E., *et al.* (2020). SARS-CoV-2 neutralizing  
801 antibody structures inform therapeutic strategies. *Nature* *588*, 682-687.  
802
- 803 Bartsch, Y., Tong, X., Kang, J., Avendaño, M.J., Serrano, E.F., García-Salum, T., Pardo-Roa,  
804 C., Riquelme, A., Medina, R.A., and Alter, G. (2021). Preserved Omicron Spike specific  
805 antibody binding and Fc-recognition across COVID-19 vaccine platforms. *medRxiv : the preprint*  
806 *server for health sciences*.  
807
- 808 Bentley, E.G., Kirby, A., Sharma, P., Kipar, A., Mega, D.F., Bramwell, C., Penrice-Randal, R.,  
809 Prince, T., Brown, J.C., Zhou, J., *et al.* (2021). SARS-CoV-2 Omicron-B.1.1.529 Variant leads to  
810 less severe disease than Pango B and Delta variants strains in a mouse model of severe  
811 COVID-19. *bioRxiv*, 2021.2012.2026.474085.  
812
- 813 Buchan, S.A., Chung, H., Brown, K.A., Austin, P.C., Fell, D.B., Gubbay, J.B., Nasreen, S.,  
814 Schwartz, K.L., Sundaram, M.E., Tadrous, M., *et al.* (2022). Effectiveness of COVID-19  
815 vaccines against Omicron or Delta infection. *medRxiv : the preprint server for health sciences*,  
816 2021.2012.2030.21268565.  
817
- 818 Cameroni, E., Bowen, J.E., Rosen, L.E., Saliba, C., Zepeda, S.K., Culap, K., Pinto, D.,  
819 VanBlargan, L.A., De Marco, A., di Iulio, J., *et al.* (2021). Broadly neutralizing antibodies  
820 overcome SARS-CoV-2 Omicron antigenic shift. *Nature*.  
821

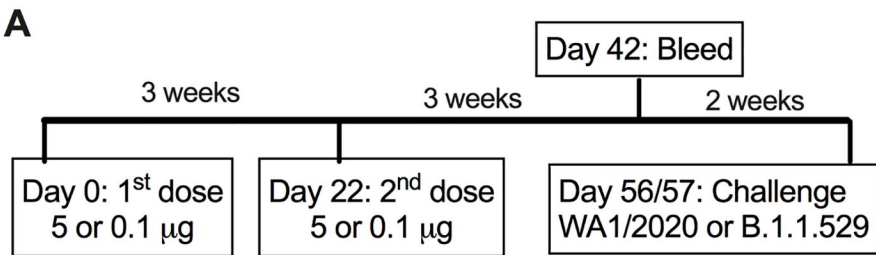
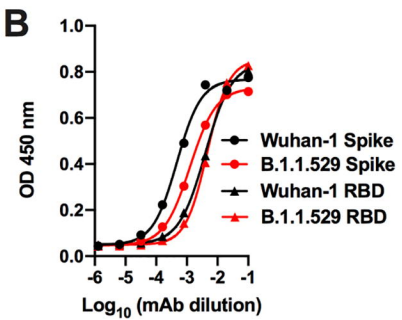
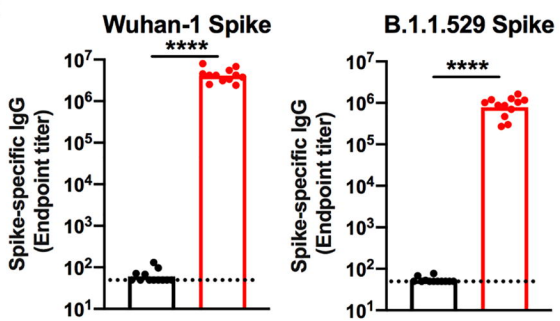
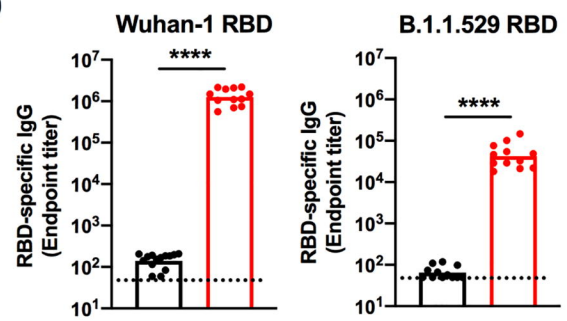
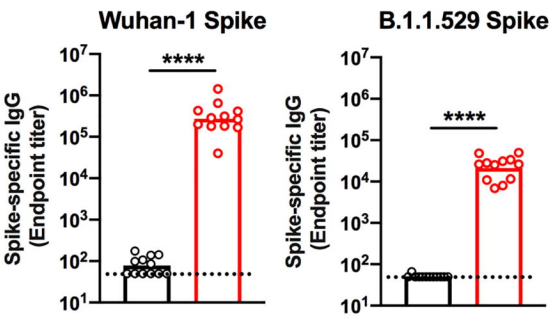
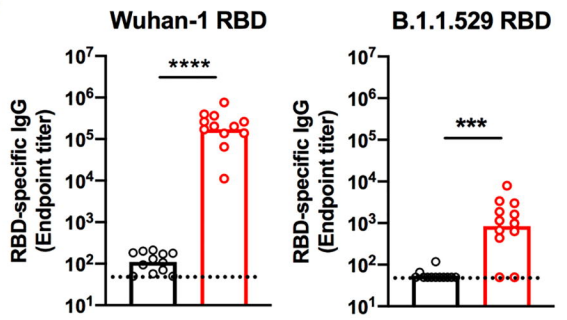
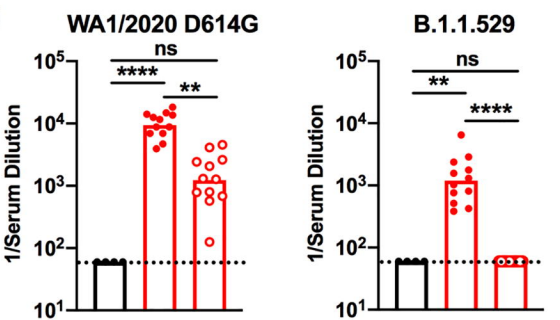
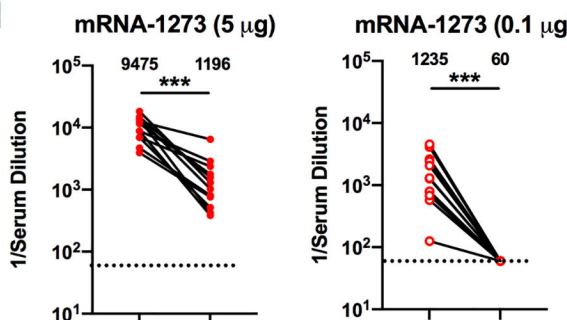
- 822 Cao, Y., Su, B., Guo, X., Sun, W., Deng, Y., Bao, L., Zhu, Q., Zhang, X., Zheng, Y., Geng, C., *et*  
823 *al.* (2020). Potent neutralizing antibodies against SARS-CoV-2 identified by high-throughput  
824 single-cell sequencing of convalescent patients' B cells. *Cell* 182, 73-84.  
825
- 826 Cao, Y., Wang, J., Jian, F., Xiao, T., Song, W., Yisimayi, A., Huang, W., Li, Q., Wang, P., An,  
827 R., *et al.* (2021). Omicron escapes the majority of existing SARS-CoV-2 neutralizing antibodies.  
828 *Nature*.  
829
- 830 Case, J.B., Bailey, A.L., Kim, A.S., Chen, R.E., and Diamond, M.S. (2020a). Growth, detection,  
831 quantification, and inactivation of SARS-CoV-2. *Virology* 548, 39-48.  
832
- 833 Case, J.B., Rothlauf, P.W., Chen, R.E., Liu, Z., Zhao, H., Kim, A., S., Bloyet, L.M., Zeng, Q.,  
834 Tahan, S., Droit, L., *et al.* (2020b). Neutralizing antibody and soluble ACE2 inhibition of a  
835 replication-competent VSV-SARS-CoV-2 and a clinical isolate of SARS-CoV-2. *Cell Host and*  
836 *Microbe* 28, 475-485.  
837
- 838 Cele, S., Jackson, L., Khan, K., Khoury, D.S., Moyo-Gwete, T., Tegally, H., Scheepers, C.,  
839 Amoako, D., Karim, F., Bernstein, M., *et al.* (2021). SARS-CoV-2 Omicron has extensive but  
840 incomplete escape of Pfizer BNT162b2 elicited neutralization and requires ACE2 for infection.  
841 medRxiv : the preprint server for health sciences, 2021.2012.2008.21267417.  
842
- 843 Chen, R.E., Gorman, M.J., Zhu, D.Y., Carreño, J.M., Yuan, D., VanBlargan, L.A., Burdess, S.,  
844 Lauffenburger, D.A., Kim, W., Turner, J.S., *et al.* (2021a). Reduced antibody activity against  
845 SARS-CoV-2 B.1.617.2 delta virus in serum of mRNA-vaccinated individuals receiving tumor  
846 necrosis factor- $\alpha$  inhibitors. *Med (New York, NY)* 2, 1327-1341.e1324.  
847
- 848 Chen, R.E., Winkler, E.S., Case, J.B., Aziati, I.D., Bricker, T.L., Joshi, A., Darling, T.L., Ying, B.,  
849 Errico, J.M., Shrihari, S., *et al.* (2021b). In vivo monoclonal antibody efficacy against SARS-  
850 CoV-2 variant strains. *Nature*.  
851
- 852 Chen, R.E., Zhang, X., Case, J.B., Winkler, E.S., Liu, Y., VanBlargan, L.A., Liu, J., Errico, J.M.,  
853 Xie, X., Suryadevara, N., *et al.* (2021c). Resistance of SARS-CoV-2 variants to neutralization by  
854 monoclonal and serum-derived polyclonal antibodies. *Nat Med*.  
855
- 856 Choi, A., Koch, M., Wu, K., Chu, L., Ma, L., Hill, A., Nunna, N., Huang, W., Oestreicher, J.,  
857 Colpitts, T., *et al.* (2021). Safety and immunogenicity of SARS-CoV-2 variant mRNA vaccine  
858 boosters in healthy adults: an interim analysis. *Nat Med* 27, 2025-2031.  
859
- 860 Christensen, P.A., Olsen, R.J., Long, S.W., Snehal, R., Davis, J.J., Ojeda Saavedra, M.,  
861 Reppond, K., Shyer, M.N., Cambric, J., Gadd, R., *et al.* (2022). Signals of significantly increased  
862 vaccine breakthrough, decreased hospitalization rates, and less severe disease in patients with  
863 COVID-19 caused by the Omicron variant of SARS-CoV-2 in Houston, Texas. medRxiv : the  
864 preprint server for health sciences, 2021.2012.2030.21268560.  
865
- 866 Corbett, K.S., Edwards, D.K., Leist, S.R., Abiona, O.M., Boyoglu-Barnum, S., Gillespie, R.A.,  
867 Himansu, S., Schäfer, A., Ziwawo, C.T., DiPiazza, A.T., *et al.* (2020). SARS-CoV-2 mRNA  
868 vaccine design enabled by prototype pathogen preparedness. *Nature* 586, 567-571.  
869
- 870 Dejnirattisai, W., Huo, J., Zhou, D., Zahradník, J., Supasa, P., Liu, C., Duyvesteyn, H.M.E.,  
871 Ginn, H.M., Mentzer, A.J., Tuekprakhon, A., *et al.* (2022). SARS-CoV-2 Omicron-B.1.1.529  
872 leads to widespread escape from neutralizing antibody responses. *Cell*.

873  
874 Edara, V.V., Manning, K.E., Ellis, M., Lai, L., Moore, K.M., Foster, S.L., Floyd, K., Davis-  
875 Gardner, M.E., Mantus, G., Nyhoff, L.E., *et al.* (2021). mRNA-1273 and BNT162b2 mRNA  
876 vaccines have reduced neutralizing activity against the SARS-CoV-2 Omicron variant. bioRxiv.  
877  
878 Elliott, P., Bodinier, B., Eales, O., Wang, H., Haw, D., Elliott, J., Whitaker, M., Jonnerby, J.,  
879 Tang, D., Walters, C.E., *et al.* (2021). Rapid increase in Omicron infections in England during  
880 December 2021: REACT-1 study. medRxiv : the preprint server for health sciences,  
881 2021.2012.2022.21268252.  
882  
883 Evans, J.P., Zeng, C., Carlin, C., Lozanski, G., Saif, L.J., Oltz, E.M., Gumina, R.J., and Liu, S.L.  
884 (2021). Loss of Neutralizing Antibody Response to mRNA Vaccination against SARS-CoV-2  
885 Variants: Differing Kinetics and Strong Boosting by Breakthrough Infection. bioRxiv.  
886  
887 Falsey, A.R., Frenck, R.W., Walsh, E.E., Kitchin, N., Absalon, J., Gurtman, A., Lockhart, S.,  
888 Bailey, R., Swanson, K.A., Xu, X., *et al.* (2021). SARS-CoV-2 Neutralization with BNT162b2  
889 Vaccine Dose 3. *New England Journal of Medicine* 385, 1627-1629.  
890  
891 Gagne, M., Moliva, J.I., Foulds, K.E., Andrew, S.F., Flynn, B.J., Werner, A.P., Wagner, D.A.,  
892 Teng, I.-T., Lin, B.C., Moore, C., *et al.* (2022). mRNA-1273 or mRNA-Omicron boost in  
893 vaccinated macaques elicits comparable B cell expansion, neutralizing antibodies and  
894 protection against Omicron. bioRxiv, 2022.2002.2003.479037.  
895  
896 Gao, Y., Cai, C., Grifoni, A., Müller, T.R., Niessl, J., Olofsson, A., Humbert, M., Hansson, L.,  
897 Österborg, A., Bergman, P., *et al.* (2022). Ancestral SARS-CoV-2-specific T cells cross-  
898 recognize the Omicron variant. *Nat Med*.  
899  
900 Graham, B.S. (2020). Rapid COVID-19 vaccine development. *Science* 368, 945-946.  
901  
902 Gu, H., Chen, Q., Yang, G., He, L., Fan, H., Deng, Y.Q., Wang, Y., Teng, Y., Zhao, Z., Cui, Y.,  
903 *et al.* (2020). Adaptation of SARS-CoV-2 in BALB/c mice for testing vaccine efficacy. *Science*  
904 369, 1603-1607.  
905  
906 Halfmann, P.J., Iida, S., Iwatsuki-Horimoto, K., Maemura, T., Kiso, M., Scheaffer, S.M., Darling,  
907 T.L., Joshi, A., Loeber, S., Singh, G., *et al.* (2022). SARS-CoV-2 Omicron virus causes  
908 attenuated disease in mice and hamsters. *Nature*.  
909  
910 Hassett, K.J., Benenato, K.E., Jacquinet, E., Lee, A., Woods, A., Yuzhakov, O., Himansu, S.,  
911 Deterling, J., Geilich, B.M., Ketova, T., *et al.* (2019). Optimization of Lipid Nanoparticles for  
912 Intramuscular Administration of mRNA Vaccines. *Molecular therapy Nucleic acids* 15, 1-11.  
913  
914 Imai, M., Iwatsuki-Horimoto, K., Hatta, M., Loeber, S., Halfmann, P.J., Nakajima, N., Watanabe,  
915 T., Ujje, M., Takahashi, K., Ito, M., *et al.* (2020). Syrian hamsters as a small animal model for  
916 SARS-CoV-2 infection and countermeasure development. *Proc Natl Acad Sci U S A* 117,  
917 16587-16595.  
918  
919 Keeton, R., Tincho, M.B., Ngomti, A., Baguma, R., Benede, N., Suzuki, A., Khan, K., Cele, S.,  
920 Bernstein, M., Karim, F., *et al.* (2022). T cell responses to SARS-CoV-2 spike cross-recognize  
921 Omicron. *Nature*.  
922

- 923 Khoury, D.S., Cromer, D., Reynaldi, A., Schlub, T.E., Wheatley, A.K., Juno, J.A., Subbarao, K.,  
924 Kent, S.J., Triccas, J.A., and Davenport, M.P. (2021). Neutralizing antibody levels are highly  
925 predictive of immune protection from symptomatic SARS-CoV-2 infection. *Nat Med* 27, 1205-  
926 1211.
- 927
- 928 Krause, P.R., Fleming, T.R., Longini, I.M., Peto, R., Briand, S., Heymann, D.L., Beral, V.,  
929 Snape, M.D., Rees, H., Ropero, A.M., *et al.* (2021). SARS-CoV-2 Variants and Vaccines. *N*  
930 *Engl J Med* 385, 179-186.
- 931
- 932 Lee, I.-J., Sun, C.-P., Wu, P.-Y., Lan, Y.-H., Wang, I.-H., Liu, W.-C., Tseng, S.-C., Tsung, S.-I.,  
933 Chou, Y.-C., Kumari, M., *et al.* (2022). Omicron-specific mRNA vaccine induced potent  
934 neutralizing antibody against Omicron but not other SARS-CoV-2 variants. *bioRxiv*,  
935 2022.2001.2031.478406.
- 936
- 937 Letko, M., Marzi, A., and Munster, V. (2020). Functional assessment of cell entry and receptor  
938 usage for SARS-CoV-2 and other lineage B betacoronaviruses. *Nature microbiology* 5, 562-569.
- 939 Liu, L., Iketani, S., Guo, Y., Chan, J.F., Wang, M., Liu, L., Luo, Y., Chu, H., Huang, Y., Nair,  
940 M.S., *et al.* (2021a). Striking Antibody Evasion Manifested by the Omicron Variant of SARS-  
941 CoV-2. *Nature*.
- 942
- 943 Liu, Y., Hu, G., Wang, Y., Ren, W., Zhao, X., Ji, F., Zhu, Y., Feng, F., Gong, M., Ju, X., *et al.*  
944 (2021b). Functional and genetic analysis of viral receptor ACE2 orthologs reveals a broad  
945 potential host range of SARS-CoV-2. *Proc Natl Acad Sci U S A* 118.
- 946
- 947 Liu, Z., VanBlargan, L.A., Bloyet, L.M., Rothlauf, P.W., Chen, R.E., Stumpf, S., Zhao, H., Errico,  
948 J.M., Theel, E.S., Liebeskind, M.J., *et al.* (2021c). Identification of SARS-CoV-2 spike mutations  
949 that attenuate monoclonal and serum antibody neutralization. *Cell Host Microbe* 29, 477-  
950 488.e474.
- 951
- 952 Munro, A.P.S., Janani, L., Cornelius, V., Aley, P.K., Babbage, G., Baxter, D., Bula, M., Cathie,  
953 K., Chatterjee, K., Dodd, K., *et al.* (2021). Safety and immunogenicity of seven COVID-19  
954 vaccines as a third dose (booster) following two doses of ChAdOx1 nCov-19 or BNT162b2 in  
955 the UK (COV-BOOST): a blinded, multicentre, randomised, controlled, phase 2 trial. *Lancet* 398,  
956 2258-2276.
- 957
- 958 Naranbhai, V., St Denis, K.J., Lam, E.C., Ofoman, O., Garcia-Beltran, W.F., Mairena, C.B.,  
959 Bhan, A.K., Gainor, J.F., Balazs, A.B., and Iafrate, A.J. (2022). Neutralization breadth of SARS-  
960 CoV-2 viral variants following primary series and booster SARS-CoV-2 vaccines in patients with  
961 cancer. *Cancer cell*.
- 962
- 963 Nelson, J., Sorensen, E.W., Mintri, S., Rabideau, A.E., Zheng, W., Besin, G., Khatwani, N., Su,  
964 S.V., Miracco, E.J., Issa, W.J., *et al.* (2020). Impact of mRNA chemistry and manufacturing  
965 process on innate immune activation. *Science advances* 6, eaaz6893.
- 966
- 967 Pajon, R., Doria-Rose, N.A., Shen, X., Schmidt, S.D., O'Dell, S., McDanal, C., Feng, W., Tong,  
968 J., Eaton, A., Magliano, M., *et al.* (2022). SARS-CoV-2 Omicron Variant Neutralization after  
969 mRNA-1273 Booster Vaccination. *N Engl J Med*.
- 970
- 971 Pinto, D., Park, Y.J., Beltramello, M., Walls, A.C., Tortorici, M.A., Bianchi, S., Jaconi, S., Culap,  
972 K., Zatta, F., De Marco, A., *et al.* (2020). Cross-neutralization of SARS-CoV-2 by a human  
973 monoclonal SARS-CoV antibody. *Nature* 583, 290-295.

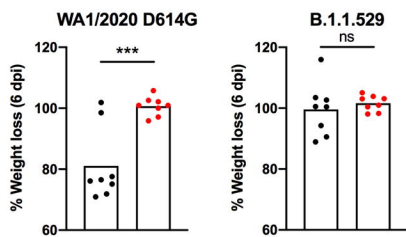
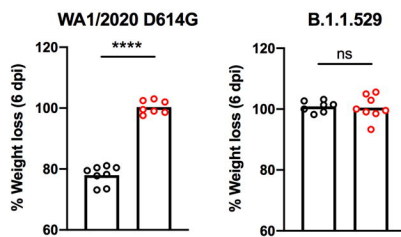
974  
975 Plante, J.A., Liu, Y., Liu, J., Xia, H., Johnson, B.A., Lokugamage, K.G., Zhang, X., Muruato,  
976 A.E., Zou, J., Fontes-Garfias, C.R., *et al.* (2020). Spike mutation D614G alters SARS-CoV-2  
977 fitness. *Nature*.  
978  
979 Rathe, J.A., Hemann, E.A., Eggenberger, J., Li, Z., Knoll, M.L., Stokes, C., Hsiang, T.Y.,  
980 Netland, J., Takehara, K.K., Pepper, M., *et al.* (2020). SARS-CoV-2 Serologic Assays in Control  
981 and Unknown Populations Demonstrate the Necessity of Virus Neutralization Testing. *J Infect*  
982 *Dis*.  
983  
984 Rathnasinghe, R., Jangra, S., Cupic, A., Martínez-Romero, C., Mulder, L.C.F., Kehrer, T., Yildiz,  
985 S., Choi, A., Mena, I., De Vriese, J., *et al.* (2021). The N501Y mutation in SARS-CoV-2 spike  
986 leads to morbidity in obese and aged mice and is neutralized by convalescent and post-  
987 vaccination human sera. *medRxiv : the preprint server for health sciences*.  
988  
989 Rössler, A., Knabl, L., Laer, D.v., and Kimpel, J. (2022). Neutralization profile of Omicron variant  
990 convalescent individuals. *medRxiv : the preprint server for health sciences*,  
991 2022.2002.2001.22270263.  
992  
993 Shuai, H., Chan, J.F., Hu, B., Chai, Y., Yuen, T.T., Yin, F., Huang, X., Yoon, C., Hu, J.C., Liu,  
994 H., *et al.* (2022). Attenuated replication and pathogenicity of SARS-CoV-2 B.1.1.529 Omicron.  
995 *Nature*.  
996  
997 Stadlbauer, D., Amanat, F., Chromikova, V., Jiang, K., Strohmeier, S., Arunkumar, G.A., Tan, J.,  
998 Bhavsar, D., Capuano, C., Kirkpatrick, E., *et al.* (2020). SARS-CoV-2 Seroconversion in  
999 Humans: A Detailed Protocol for a Serological Assay, Antigen Production, and Test Setup. *Curr*  
1000 *Protoc Microbiol* 57, e100.  
1001  
1002 Tortorici, M.A., Beltramello, M., Lempp, F.A., Pinto, D., Dang, H.V., Rosen, L.E., McCallum, M.,  
1003 Bowen, J., Minola, A., Jaconi, S., *et al.* (2020). Ultrapotent human antibodies protect against  
1004 SARS-CoV-2 challenge via multiple mechanisms. *Science* 370, 950-957.  
1005  
1006 VanBlargan, L.A., Adams, L.J., Liu, Z., Chen, R.E., Gilchuk, P., Raju, S., Smith, B.K., Zhao, H.,  
1007 Case, J.B., Winkler, E.S., *et al.* (2021). A potently neutralizing SARS-CoV-2 antibody inhibits  
1008 variants of concern by utilizing unique binding residues in a highly conserved epitope. *Immunity*.  
1009  
1010 VanBlargan, L.A., Errico, J.M., Halfmann, P.J., Zost, S.J., Crowe, J.E., Jr., Purcell, L.A.,  
1011 Kawaoka, Y., Corti, D., Fremont, D.H., and Diamond, M.S. (2022). An infectious SARS-CoV-2  
1012 B.1.1.529 Omicron virus escapes neutralization by therapeutic monoclonal antibodies. *Nat Med*,  
1013 1-6.  
1014  
1015 Waltz, E. (2022). Does the world need an Omicron vaccine? What researchers say. *Nature*.  
1016  
1017 Wang, Z., Muecksch, F., Schaefer-Babajew, D., Finkin, S., Viant, C., Gaebler, C., Hoffmann,  
1018 H.H., Barnes, C.O., Cipolla, M., Ramos, V., *et al.* (2021). Naturally enhanced neutralizing  
1019 breadth against SARS-CoV-2 one year after infection. *Nature* 595, 426-431.  
1020  
1021 Whitt, M.A. (2010). Generation of VSV pseudotypes using recombinant  $\Delta$ G-VSV for studies on  
1022 virus entry, identification of entry inhibitors, and immune responses to vaccines. *J Virol Methods*  
1023 169, 365-374.  
1024

- 1025 Widge, A.T., Rouphael, N.G., Jackson, L.A., Anderson, E.J., Roberts, P.C., Makhene, M.,  
1026 Chappell, J.D., Denison, M.R., Stevens, L.J., Pruijssers, A.J., *et al.* (2021). Durability of  
1027 Responses after SARS-CoV-2 mRNA-1273 Vaccination. *N Engl J Med* 384, 80-82.  
1028  
1029 Wilhelm, A., Widera, M., Grikscheit, K., Toptan, T., Schenk, B., Pallas, C., Metzler, M., Kohmer,  
1030 N., Hoehl, S., Helfritz, F.A., *et al.* (2021). Reduced Neutralization of SARS-CoV-2 Omicron  
1031 Variant by Vaccine Sera and monoclonal antibodies. medRxiv : the preprint server for health  
1032 sciences, 2021.2012.2007.21267432.  
1033  
1034 Winkler, E.S., Bailey, A.L., Kafai, N.M., Nair, S., McCune, B.T., Yu, J., Fox, J.M., Chen, R.E.,  
1035 Earnest, J.T., Keeler, S.P., *et al.* (2020). SARS-CoV-2 infection of human ACE2-transgenic  
1036 mice causes severe lung inflammation and impaired function. *Nat Immunol* 21, 1327-1335.  
1037  
1038 Wu, K., Werner, A.P., Koch, M., Choi, A., Narayanan, E., Stewart-Jones, G.B.E., Colpitts, T.,  
1039 Bennett, H., Boyoglu-Barnum, S., Shi, W., *et al.* (2021). Serum Neutralizing Activity Elicited by  
1040 mRNA-1273 Vaccine. *N Engl J Med* 384, 1468-1470.  
1041  
1042 Ying, B., Whitener, B., VanBlargan, L.A., Hassan, A.O., Shrihari, S., Liang, C.Y., Karl, C.E.,  
1043 Mackin, S., Chen, R.E., Kafai, N.M., *et al.* (2021). Protective activity of mRNA vaccines against  
1044 ancestral and variant SARS-CoV-2 strains. *Sci Transl Med*, eabm3302.  
1045  
1046 Zang, R., Gomez Castro, M.F., McCune, B.T., Zeng, Q., Rothlauf, P.W., Sonnek, N.M., Liu, Z.,  
1047 Brulois, K.F., Wang, X., Greenberg, H.B., *et al.* (2020). TMPRSS2 and TMPRSS4 promote  
1048 SARS-CoV-2 infection of human small intestinal enterocytes. *Sci Immunol* 5.  
1049  
1050 Zost, S.J., Gilchuk, P., Chen, R.E., Case, J.B., Reidy, J.X., Trivette, A., Nargi, R.S., Sutton,  
1051 R.E., Suryadevara, N., Chen, E.C., *et al.* (2020). Rapid isolation and profiling of a diverse panel  
1052 of human monoclonal antibodies targeting the SARS-CoV-2 spike protein. *Nat Med* 26, 1422-  
1053 1427.  
1054

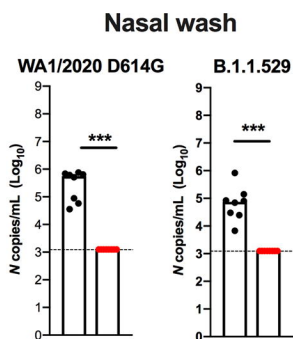
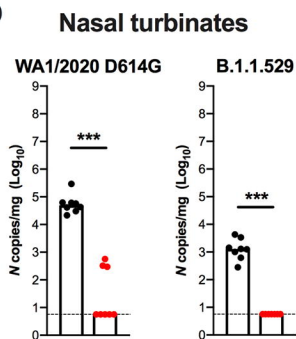
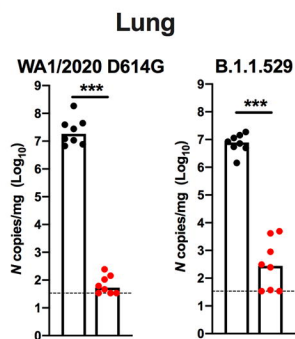
**A****B****C****D****E****F****G****H**

● Control (5 μg) ● mRNA-1273 (5 μg) ○ Control (0.1 μg) ○ mRNA-1273 (0.1 μg)

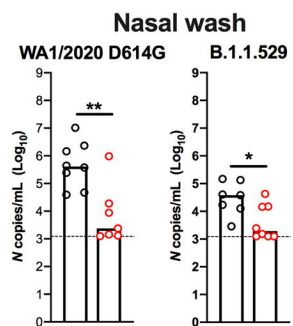
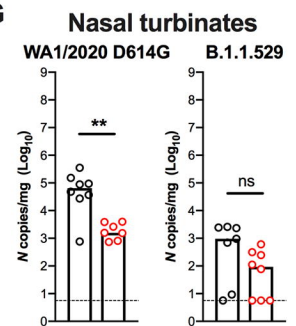
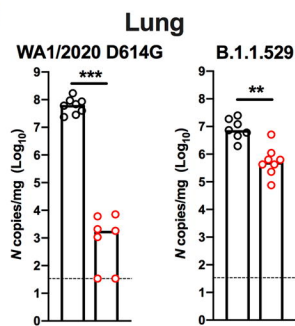


**A****B**

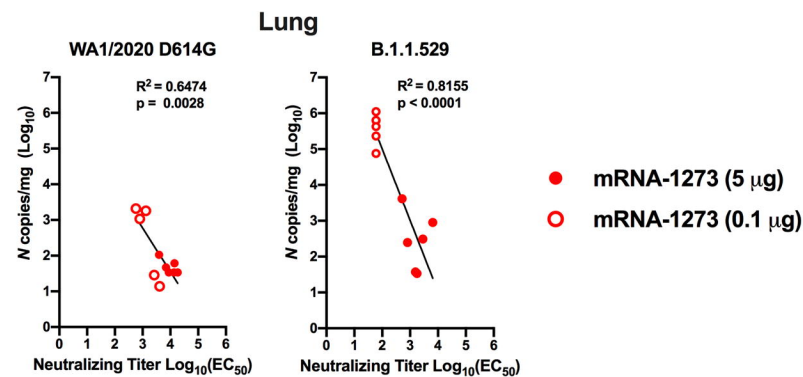
- Control (5 µg)
- mRNA-1273 (5 µg)
- Control (0.1 µg)
- mRNA-1273 (0.1 µg)

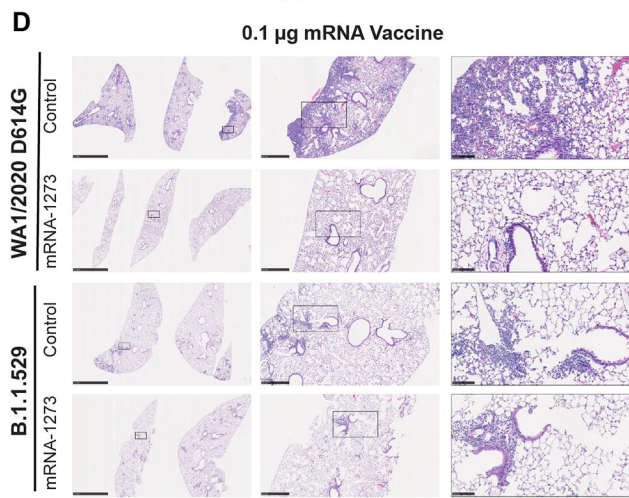
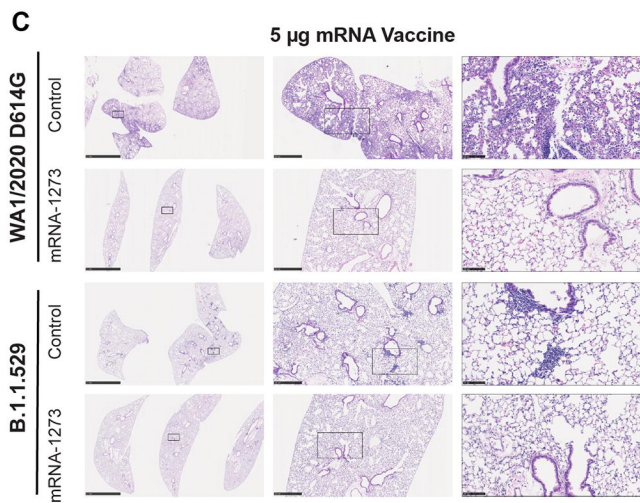
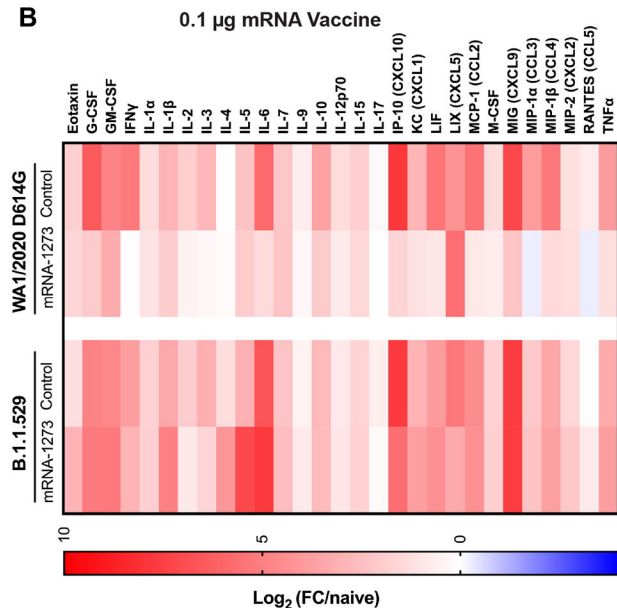
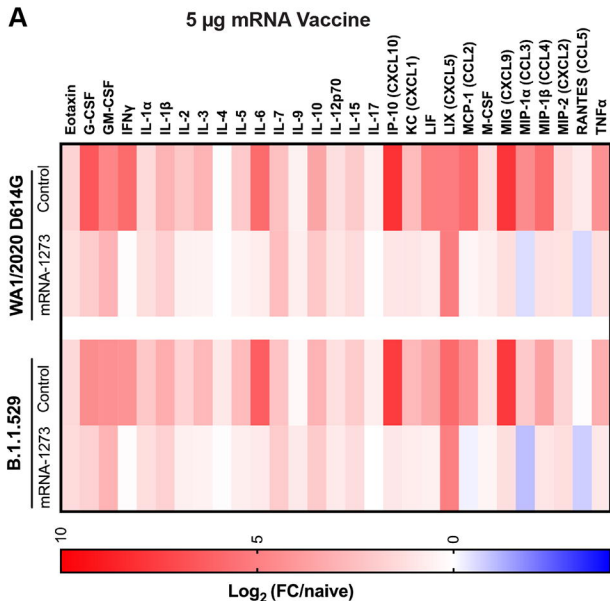
**C****D****E**

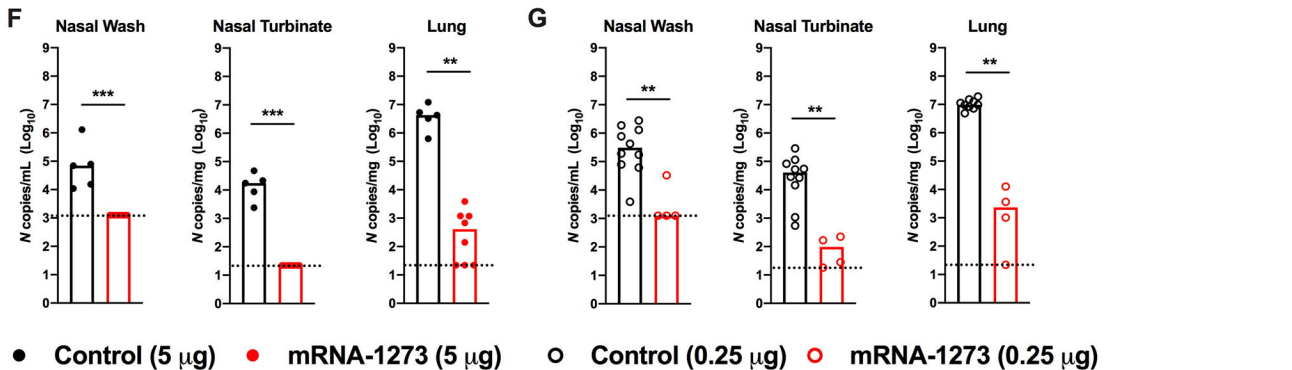
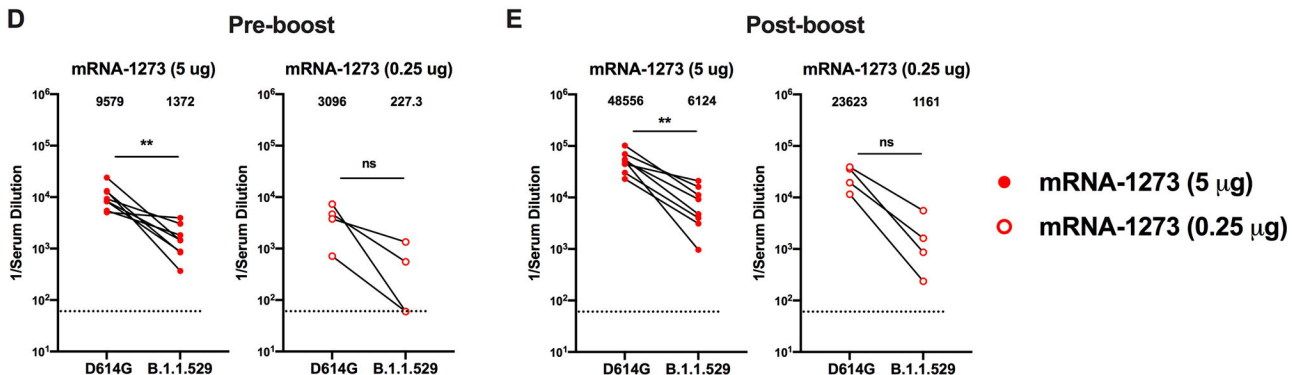
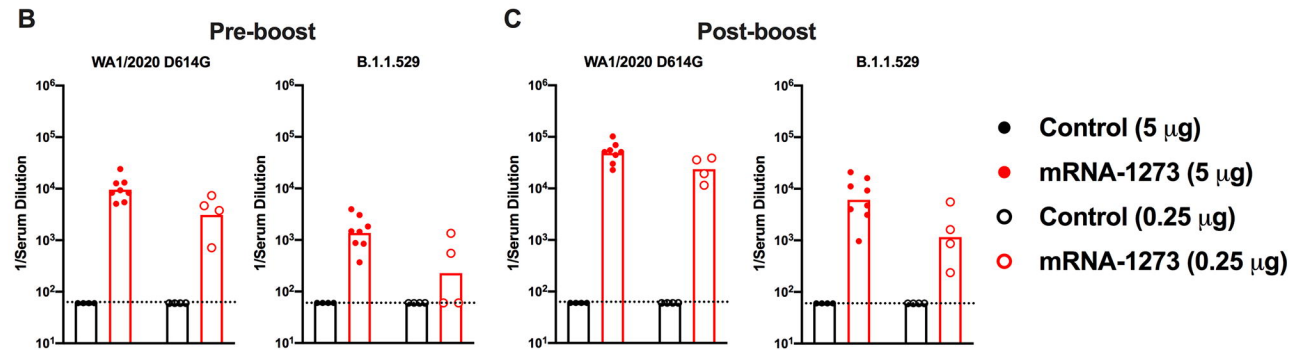
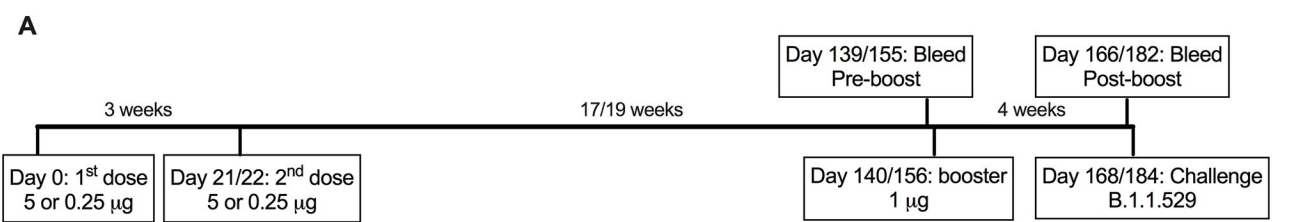
- Control (5 µg)
- mRNA-1273 (5 µg)

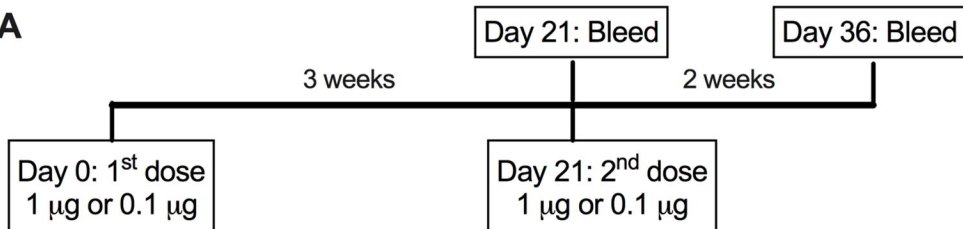
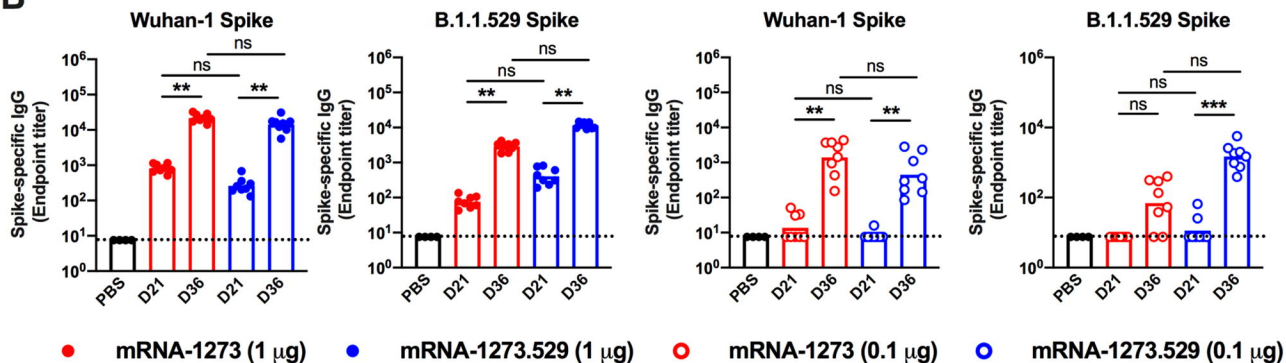
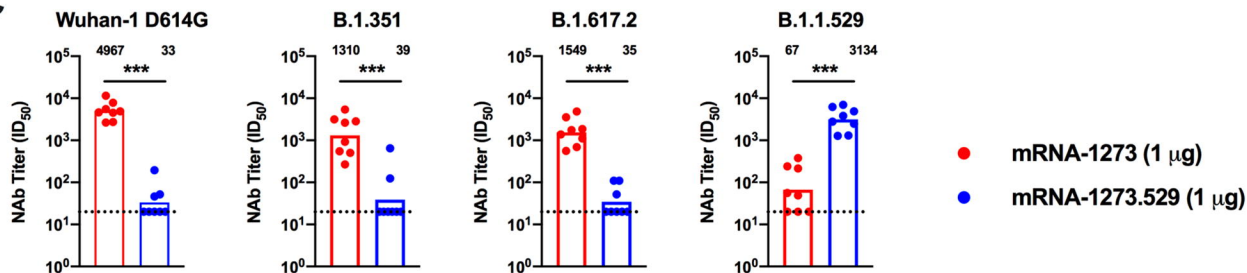
**F****G****H**

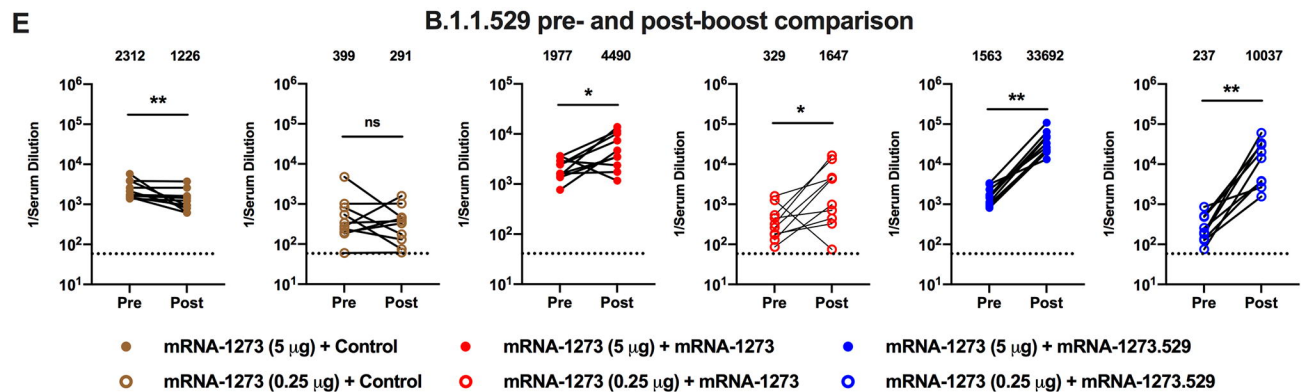
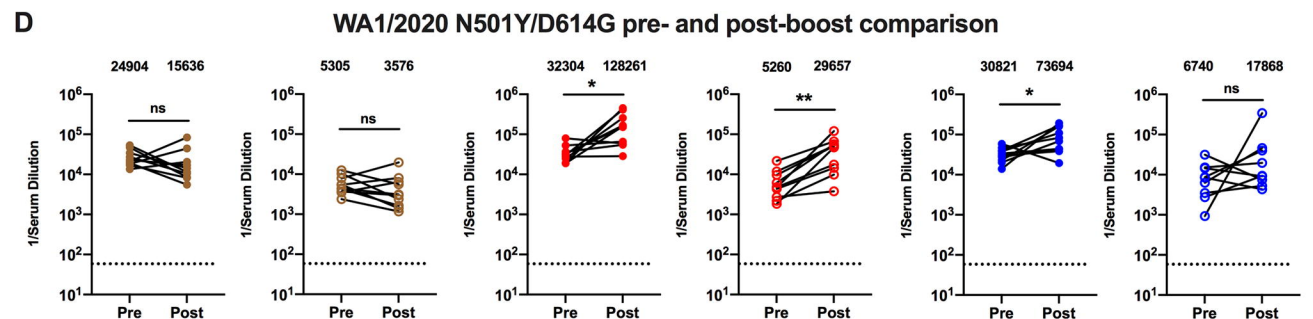
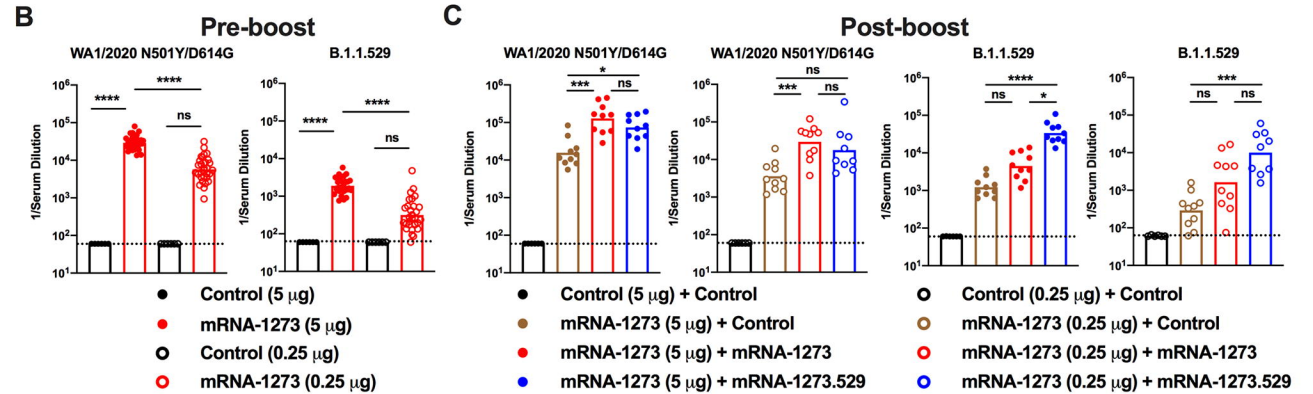
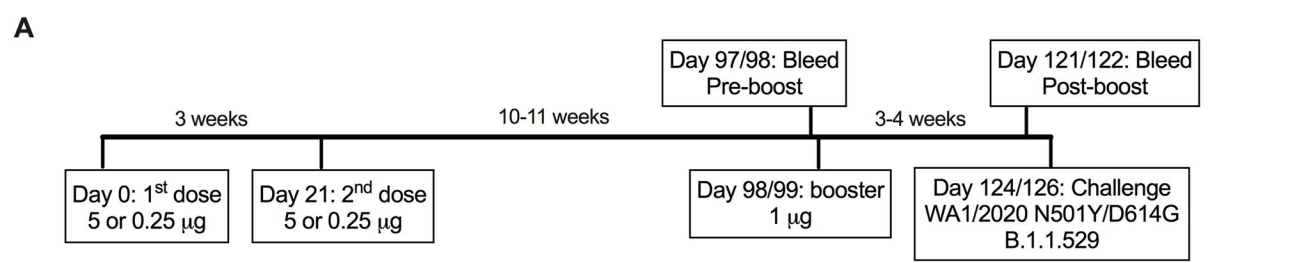
- Control (0.1 µg)
- mRNA-1273 (0.1 µg)

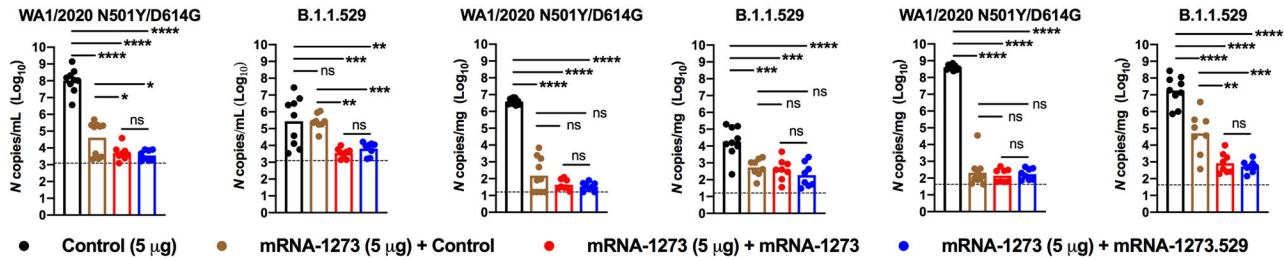
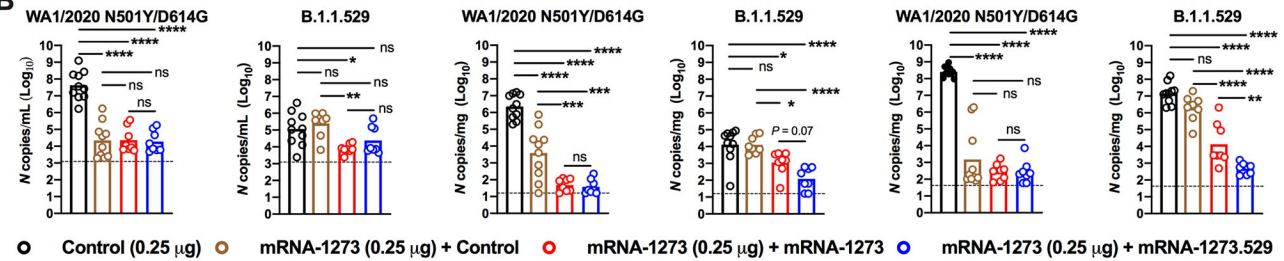
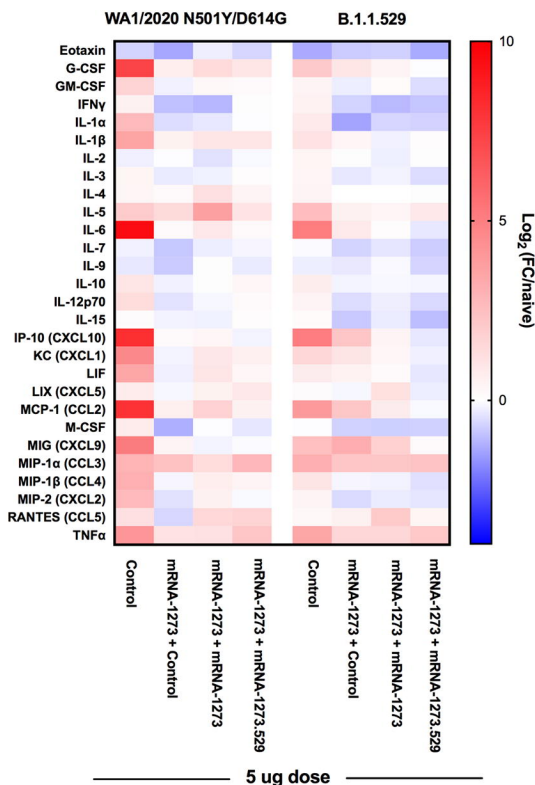
**I**





**A****B****C**



**A****Nasal wash****Nasal turbinates****Lung****B****C****D**